SPECIFIC SENSORY NEURONS AND INSULIN-LIKE PEPTIDES MODULATE FOOD TYPE-DEPENDENT OOGENESIS AND FERTILIZATION IN *CAENORHABDITIS ELEGANS*

Shashwat Mishra[1], Mohamed Dabaja[1], Asra Akhlaq[1], Bianca Pereira[1], Kelsey Marbach[1], Mediha Rovcanin[1], Rashmi Chandra[1], Antonio Caballero[2], Diana Fernandes de Abreu[2], QueeLim Ch'ng[2], Joy Alcedo[1,*]

[1]Department of Biological Sciences, Wayne State University, Detroit, Michigan, USA

[2]Centre for Developmental Neurobiology, King's College London, London, UK

*Correspondence to: joy.alcedo@wayne.edu

Abstract

An animal's responses to environmental cues are critical for its reproductive program. Thus, a mechanism that allows the animal to sense and adjust to its environment should make for a more efficient reproductive physiology. Here we demonstrate that in *Caenorhabditis elegans* specific sensory neurons influence onset of oogenesis through insulin signaling in response to food-derived cues. The chemosensory neurons ASJ modulate oogenesis onset through the insulin-like peptide (ILP) INS-6. In contrast, other sensory neurons, the olfactory neurons AWA, regulate food type-dependent differences in *C. elegans* fertilization rates, but not onset of oogenesis. AWA modulates fertilization rates at least partly in parallel to insulin receptor signaling, since the insulin receptor DAF-2 regulates fertilization independently of food type, which requires ILPs other than INS-6. Together our findings suggest that optimal reproduction requires the integration of diverse food-derived inputs through multiple neuronal signals acting on the *C. elegans* germline.

15 **Introduction**

16 The survival of an individual and its species involves reproductive mechanisms that are
17 subject to food-dependent modulation. In the worm *C. elegans*, sensory neurons influence
18 food-dependent survival (***Maier et al., 2010***) and germline physiology (***Dalfo et al., 2012;***
19 ***Sowa et al., 2015; Aprison and Ruvinsky, 2017; Perez et al., 2021***). This suggests the
20 intriguing possibility that sensory perception optimizes survival by modulating the germline
21 in a given environment, which makes it important to understand how the sensory system
22 affects germ cells.

23 In the germline of the *C. elegans* hermaphrodite, germ cells first undergo
24 spermatogenesis, before switching to oogenesis [***Figure 1A***; reviewed by (***Kimble and***
25 ***Crittenden, 2007***)]. After oogenesis begins, oocytes undergo arrest at the diakinesis
26 stage of prophase I [reviewed by (***Greenstein, 2005***)]. Oocytes are released from this
27 arrest in an assembly-line manner by a hormone secreted from sperm, where the oocyte
28 most proximal to the spermatheca matures first (***McCarter et al., 1999; Miller et al.,***
29 ***2001***). Once released from arrest, the oocyte is also immediately ovulated into the
30 spermatheca, where it is fertilized by a sperm (***McCarter et al., 1999; Miller et al., 2001***).
31 Thus, in *C. elegans* hermaphrodites, the rate of oocyte maturation determines the rate of
32 fertilization (***McCarter et al., 1999***).

33 Some of the *C. elegans* sensory neurons have been shown to modulate germ cell
34 proliferation (***Dalfo et al., 2012; Aprison and Ruvinsky, 2017***) and oocyte senescence
35 (***Sowa et al., 2015***) in response to food or pheromones. However, it remains unclear
36 whether the same sensory neurons regulate germline differentiation and fertilization or
37 what signaling mechanisms underlie these sensory influences.

38 Insulin signaling could mediate the sensory responses to food [reviewed by (***Allen***
39 ***et al., 2015***)]. Worms have 40 insulin-like peptides [ILPs; (***Duret et al., 1998; Kawano et***
40 ***al., 2000; Pierce et al., 2001; Li et al., 2003***), many of which are expressed in sensory

41 neurons and could act alone or combinatorially to regulate several physiological programs
42 (***Cornils et al., 2011; Chen et al., 2013; Ritter et al., 2013; Fernandes de Abreu et al.,***
43 ***2014***). Indeed, two ILPs, *ins-3* and *ins-33*, have already been shown to regulate germ cell
44 proliferation (***Michaelson et al., 2010***); however, the cells that secrete these signals that
45 affect the germline are unknown.

46 In this study, we find that specific sensory neurons and ILPs regulate the timing of
47 oogenesis and fertilization through food type-dependent and -independent mechanisms.
48 In response to a specific food type, we show that the chemosensory neuron ASJ promotes
49 early oogenesis. This ASJ-dependent effect on oogenesis involves ASJ-specific
50 expression of the ILP *ins-6*. In contrast, an olfactory neuron, AWA, regulates food type-
51 dependent fertilization rates through mechanisms that differ from insulin receptor
52 signaling. The insulin receptor pathway alters fertilization rates independent of food cues
53 and employs other ILPs. Thus, our work demonstrates that oogenesis onset and
54 fertilization are subject to different ILP signals and sensory neuron activities, which ensure
55 optimal reproduction within a changing environment.

56

57 **Results**

58 **The bacterial food source modulates onset of oogenesis and fertilization rate in *C.***
59 ***elegans***

60 Previously, we have shown that different *E. coli* strains that serve as food for *C. elegans*
61 can modulate the animals' reproductive physiology, independent of their somatic
62 development (***Maier et al., 2010***). Wild-type *C. elegans* fed two different *E. coli* strains,
63 OP50 and CS180, developed through four larval stages (L1 to L4; ***Figure 1A***) at about
64 the same rate (***Figure 1B***), before they molted into young adults. However, *C.*
65 *elegans* grown on CS180 produced fewer progeny when compared to animals grown on
66 OP50 (***Figure 1C***, ***Figure 1—supplement 1***). This CS180-dependent phenotype was not

67 because the animals had restricted food intake, since they showed no delay in
68 developmental rates (***Figure 1B***). In fact, CS180-fed animals exhibited faster fertilization
69 rates during the first 24 hours of adulthood (***Figure 1D***, ***Figure 1—supplement 1***), which
70 is opposite of what would be expected for food level-restricted animals (***Maier et al., 2010***).
71 In *C. elegans*, the total number of sperm made before the gametogenesis switch
72 to oogenesis can limit the number of progeny (***Ward and Carrel, 1979***). Consistent with
73 this idea, animals fed CS180 not only had fewer progeny (***Figure 1C***, ***Figure 1—***
74 ***supplement 1***), but also fewer sperm than animals on OP50 (***Figure 1E***). To test the
75 hypothesis that the lower sperm number in *C. elegans* on CS180 was because of an earlier
76 switch from spermatogenesis to oogenesis, we examined when the oogenesis
77 marker *lin-41::GFP* (***Spike et al., 2014; Noble et al., 2016***) was first expressed (***Figure***
78 ***1F to H, Figure 1—supplement 1***). We found that a significant fraction of worms on
79 CS180 began to express the oogenesis marker *lin-41::GFP* at the mid-L4 stage, which
80 was before the marker was observed in any worms on OP50 (***Figure 1H***, ***Figure 1—***
81 ***supplement 1***). Worms fed OP50 started to express *lin-41::GFP* only at late L4 (34%),
82 when most animals on CS180 (69%) had already expressed the GFP marker (***Figure 1H***,
83 ***Figure 1—supplement 1***). To confirm further the effect of the CS180 diet on oogenesis,
84 we also analyzed the initial expression of a second oogenesis reporter, *oma-1::GFP*
85 (***Detwiler et al., 2001; Lin, 2003***), on CS180 or OP50. Similar to what we observed with
86 *lin-41::GFP*, worms fed CS180 started to express *oma-1::GFP* at mid-L4 (20%), again
87 before any OP50-fed worms (***Figure 1I***, ***Figure 1—supplement 1***). The gonads of
88 CS180-fed animals also had more arrested oocytes than the gonads of age-matched
89 adults on OP50 (***Figure 1J***). Thus, our data are consistent with the hypothesis that the
90 fewer progeny on CS180 can reflect earlier oogenesis on this food source. Together with
91 the increased rate of fertilization in CS180-fed animals (***Figure 1D***, ***Figure 1—***

92 ***supplement 1***), which would depend on the oocyte maturation rate (***McCarter et al.,***
93 ***1999***), our data suggest that CS180 promotes earlier and faster oocyte development.
94
95 **CS180-derived cues that affect oocyte development are absent from the K-12 HT115**
96 **bacteria and *Serratia marcescens***
97 OP50 is derived from an *E. coli* B strain (***Brenner, 1974***); CS180, from an *E. coli* K-12
98 strain (***Pradel et al., 1992***). One of the differences between the two bacterial strains is the
99 outer core structures of the lipopolysaccharides (LPS) on their cell walls [(***Maier et al.,***
100 ***2010***) and references therein]. The OP50 LPS is shorter than the CS180 LPS [***Figure 2A***;
101 (***Maier et al., 2010***)]. To test if this difference in LPS alters oogenesis onset and fertilization
102 rate, we examined wild-type *C. elegans* oocyte development on *E. coli* CS2429, which is
103 a K-12 strain that is derived from CS180 but has a truncated LPS [***Figure 2A***; (***Pradel et***
104 ***al., 1992; Zhang et al., 2006***)]. Interestingly, like on CS180, worms on CS2429 still
105 displayed a lower number of progeny (***Figure 2B, Figure 2—supplement 1***), early
106 oogenesis (***Figure 2C, Figure 2—supplement 1***), and faster fertilization (***Figure 2D,***
107 ***Figure 2—supplement 1***). This indicates that this difference in LPS structure is
108 insufficient to affect oocyte development.
109 Since CS180 is an *E. coli* K-12 strain, we then asked if other K-12 bacteria elicit
110 the same oocyte physiological responses. While worms on the *E. coli* K-12 HT115 bacteria
111 (***Takiff et al., 1989; Dasgupta et al., 1998***) produced a similar number of progeny as
112 worms fed CS180 (***Figure 2—supplement 1***), HT115-fed worms did not exhibit an early
113 oogenesis onset (***Figure 2E, Figure 2—supplement 1***) or faster fertilization rates (***Figure***
114 ***2F, Figure 2—supplement 1***). This suggests that the cue(s) that cause early oogenesis
115 and faster fertilization (i) might differ from the cue(s) that modulate an animal's number of
116 progeny and (ii) are specific to CS180 and its derivative CS2429.

117 Thus, we explored the potential nature of the CS180-derived cue(s) that affect
118 oocyte physiology and supplemented OP50-fed worms with CS180-conditioned media.
119 We found that these animals showed early expression of the oogenesis marker at mid-L4
120 and had faster fertilization rates, which are unlike the unsupplemented OP50-fed controls
121 (***Figure 2G and H, Figure 2—supplement 1***). However, filtration of the CS180-
122 conditioned media through a nylon membrane, which has a 0.45 μm-diameter pore size,
123 removed the cue(s) that promote early oocyte development and fast fertilization (***Figure***
124 ***2G and H, Figure 2—supplement 1***). Because the cue(s) were lost by filtration through
125 the nylon membrane filters (***Hasegawa et al., 2003***), the CS180-derived cue(s) that
126 modulate oocyte physiology are unlikely to be small molecules, such as free metabolites.
127 Because it remains possible that the CS180-derived cue(s) stimulate *C. elegans*
128 innate immunity, which in turn modulate oocyte fate and physiology, we also exposed wild-
129 type worms to two strains of the more pathogenic bacteria *Serratia marcescens* (***Pradel***
130 ***et al., 2007***). The absence of early oogenesis onset on *Serratia marcescens* (***Figure 2I,***
131 ***Figure 2—supplement 1***) suggest that the CS180 responses are not general innate
132 immune responses. Our findings also show that bacterial pathogenicity is insufficient to
133 promote earlier oocyte development.
134

135 **Food type modulates oogenesis onset and fertilization rate at different critical**
136 **periods during development**

137 To identify the critical periods for food type-dependent effects on onset of oogenesis and
138 on fertilization, we grew worms on one food type and switched them to the second food
139 type at different stages of larval development. Worms that were switched from OP50 to
140 CS180 at the first larval stage (L1; ***Figure 3—supplement 1***) or at the early part of the
141 third larval stage (L3) behaved like worms that were fed CS180 continuously (***Figure 3A***
142 ***and B, Figure 3—supplement 1***). These worms produced less progeny (***Figure 3A,***

143 ***Figure 3—supplement 1***) and expressed the oogenesis reporter earlier than animals
144 grown continuously on OP50 (***Figure 3B, Figure 3—supplement 1***). Since the germ cells
145 of worms transferred to CS180 still responded to this food source, this suggests that the
146 germ cell decision to switch to oogenesis occurs after early L3.

147 In contrast, animals that were transferred from OP50 to CS180 at late L3 or later
148 developmental stages showed the phenotype of animals that were always grown on OP50
149 (***Figure 3A and B, Figure 3—supplement 1***), which suggests that the germ cell decision
150 to switch to oogenesis has already been made by late L3. This is further supported by our
151 findings that the germ cells of worms that underwent the reciprocal switch from CS180 to
152 OP50 responded consistently to OP50 only until early L3, but not at later stages (***Figure***
153 ***3A and B, Figure 3—supplement 1***). Thus, food type can only modulate onset of
154 oogenesis before late L3, consistent with a prior study that showed that germ cell fate
155 determination occurs during this stage (***Barton and Kimble, 1990***).

156 However, the critical window for the food-type effect on fertilization rate is after the
157 early part of the fourth larval stage (L4; ***Figure 3C to F, Figure 3—supplement 1***). Worms
158 switched between one food source to the second food source at early L4 (***Figure 3D,***
159 ***Figure 3—supplement 1***) had the same fertilization rates as animals consistently fed the
160 second food source. Animals switched at mid-L4 had a delayed and less robust fertilization
161 response to the second food source (***Figure 3E, Figure 3—supplement 1***), whereas a
162 food switch immediately after the molt into adulthood had no effect on fertilization rates
163 (***Figure 3F, Figure 3—supplement 1***). Thus, fertilization rate is influenced by food type
164 until just before *C. elegans* molts into a young adult.

165

166 **A specific sensory neuron regulates the food-type differences in total progeny**

167 We have previously shown that sensory perception of food type can alter *C.*
168 *elegans* longevity (***Maier et al., 2010***), which led us to hypothesize that sensory neurons

169 will also influence the number of progeny the animals produce on the different food
170 sources. Accordingly, we tested mutants that impaired different subsets of sensory
171 neurons. Unlike wild type, the *osm-3* mutant, which has many defective sensory neurons
172 (***Tabish et al., 1995; Taylor et al., 2021***), produced the same number of offspring on both
173 OP50 and CS180 (***Figure 4A, Figure 4—supplement 1***). This suggests that at least
174 some of the *osm-3*-expressing neurons alter the worm's total progeny in response to food
175 type.

176 Similar to *osm-3* mutants, a mutation in the guanylyl cyclase gene *odr-1*, which
177 impairs a different subset of sensory neurons (***L'Etoile and Bargmann, 2000; Taylor et***
178 ***al., 2021***), also produced the same number of progeny on OP50 and CS180 (***Figure 4A,***
179 ***Figure 4—supplement 1***). However, unlike *osm-3* and *odr-1* mutants, but like wild type,
180 a defect in the transcription factor gene *odr-7*, which causes the specific loss of the
181 olfactory neuron AWA (***Sengupta et al., 1994***), led to more progeny on OP50 than on
182 CS180 (***Figure 4A, Figure 4—supplement 1***). This suggests that there is some neuronal
183 specificity in the regulation of total progeny.

184 *osm-3* and *odr-1* mutants share defects in several sensory neurons, including ASI,
185 ASJ and ASK (***Tabish et al., 1995; L'Etoile and Bargmann, 2000; Taylor et al., 2021***).
186 Individual ablation of the ASI and ASK neurons did not abolish the food type-dependent
187 differences in total progeny (***Figure 4A, Figure 4—supplement 1***). Interestingly, loss of
188 the ASJ neurons suppressed the differences in progeny number (***Figure 4A, Figure 4—***
189 ***supplement 1***) on OP50 versus CS180. Thus, our data show that, unlike ASI, ASK and
190 AWA, the neuron ASJ modulates the worm's total progeny in response to food cues.

191

192 **The ILP *ins-6* also regulates food-type differences in total progeny**

193 The number of *C. elegans* progeny is also subject to regulation by insulin signaling
194 [reviewed by (***Murphy and Hu, 2013***)], which led us to test whether insulin signaling will

195 modulate the food-type differences in progeny number. Reduction-of-function mutations
196 in *daf-2*, the *C. elegans* insulin-like growth factor receptor (***Kimura et al., 1997; Gems et***
197 ***al., 1998***), reduced or abolished the food-type differences in total progeny (***Figure 4B,***
198 ***Figure 4—supplement 1***). In contrast, a loss-of-function mutation in *daf-16*, the FOXO-
199 like transcription factor that is antagonized by DAF-2 (***Lin et al., 1997; Ogg et al., 1997***),
200 still led to food-type differences in the number of progeny on OP50 and CS180 (***Figure***
201 ***4B and E, Figure 4—supplement 1***). Together these findings indicate that insulin
202 signaling regulates total progeny in response to food cues.

203 Because ASJ neurons express at least three potential ILP ligands for the DAF-2
204 receptor, INS-1 (***Kodama et al., 2006; Tomioka et al., 2006***), INS-6 (***Cornils et al., 2011***)
205 and DAF-28 (***Li et al., 2003; Taylor et al., 2021***), we tested the effects of these three
206 peptides on progeny number. Deletion of either *ins-1* or *daf-28* did not alter the OP50- or
207 CS180-dependent progeny number (***Figure 4C, Figure 4—supplement 1***). However,
208 *ins-6* deletion mutants lost the food-type differences in total progeny (***Figure 4D and E,***
209 ***Figure 4—supplement 1***), which were restored when *daf-16* was also deleted (***Figure***
210 ***4E, Figure 4—supplement 1***). Together these data suggest that there are specific ILPs,
211 such as INS-6, that modulate food type-dependent total progeny, which depend on the
212 insulin pathway transcription factor DAF-16.

213

214 **ASJ sensory neurons promote early oogenesis on a CS180 bacterial diet**

215 Since sensory neurons modulate total progeny (***Figure 4A, Figure 4—supplement 1***),
216 we next asked whether the same sensory neurons will also alter the timing of oogenesis
217 in response to food-derived cues. We compared in parallel the onset of oogenesis in
218 *osm-3* mutants and in animals lacking their ASI or ASJ neurons.

219 Similar to the loss of food-type differences in its total progeny (***Figure 4A, Figure***
220 ***4—supplement 1***), *osm-3* mutants failed to exhibit early oogenesis on CS180 during mid-

221 L4 (***Figure 5A, Figure 5—supplement 1***). This suggests that there are *osm-3*-expressing
222 neurons that promote early oogenesis onset in response to food cues. In contrast, worms
223 lacking ASI neurons showed early oogenesis during mid-L4 (***Figure 5A, Figure 5—***
224 ***supplement 1***). Yet, the continued low level of oogenesis during late L4 in ASI-ablated
225 worms on CS180 might suggest that ASI plays a minor role in oogenesis and that the
226 food-type differences in total progeny can be uncoupled from the food-type differences in
227 oogenesis onset.

228 More importantly, ASJ-ablated worms showed no early expression of the
229 oogenesis marker *lin-41::GFP* at mid-L4 and decreased *lin-41::GFP* even during late L4
230 and lethargus (***Figure 5A, Figure 5—supplement 1***). ASJ-ablated worms also did not
231 show any mid-L4 expression of a second oogenesis marker*, oma-1::GFP*, which was
232 again different from controls (***Figure 5E, Figure 5—supplement 1***). Thus, loss of ASJ
233 delayed oogenesis based on the temporal expression of the two oogenesis reporters,
234 *lin-41::GFP* and *oma-1::GFP*. These findings demonstrate that ASJ neurons not only
235 modulate the animal's number of progeny, but also play a major role in promoting early
236 oogenesis.

237

238 ***ins-6* promotes food type-dependent early oogenesis independent of the**
239 ***daf-16*/FOXO transcription factor**

240 How does ASJ promote oogenesis? Again, the ILPs expressed by ASJ are good
241 candidates through which ASJ affects this process, since insulin signaling is an important
242 regulator of oocyte development across metazoans [reviewed by (***Das and Arur, 2017***)].
243 Indeed, both *daf-2* reduction-of-function mutants lost the early expression of the oogenesis
244 marker *lin-41::GFP* on CS180 (***Figure 5B, Figure 5—supplement 1***), whereas *daf-16*
245 deletion mutants continued to have early oogenesis on CS180 (***Figure 5C, Figure 5—***

246 ***supplement 1***). Together these observations suggest that insulin signaling also mediates
247 the food-type effects on worm oogenesis.

248 To determine whether the same ILP that regulates total progeny again regulates
249 the timing of oogenesis, we assayed the effects of *ins-6* on oogenesis and compared these
250 to the effects of *ins-1* and *daf-28*. Similar to their lack of effect on food type-dependent
251 total progeny (***Figure 4C, Figure 4—supplement 1***), the deletion of *ins-1* or *daf-28* had
252 no effect on the OP50- or CS180-dependent onset of oogenesis (***Figure 5D, Figure 5—***
253 ***supplement 1***). However, *ins-6* mutants had no early expression of *lin-41::GFP* (***Figure***
254 ***5D and F, Figure 5—supplement 1***) or *oma-1::GFP* (***Figure 5E, Figure 5—supplement***
255 ***1***) at mid-L4 on CS180. Thus, our data show that of the three ILPs tested, *ins-6* alone is
256 sufficient to modulate the food type-dependent onset of oogenesis (***Figures 5 and 6***).

257 Surprisingly, however, the lack of early oogenesis at mid-L4 in *ins-6* mutants
258 cannot be rescued by the loss of *daf-16* (***Figure 5F, Figure 5—supplement 1***), which
259 suggests that *ins-6* modulates early oogenesis independent of *daf-16*. This is reminiscent
260 of the *daf-16*-independence of *daf-2* in promoting germline meiotic progression in
261 response to food availability (**Lopez et al., 2013**). The *daf-16*-independence *of ins-6* in
262 regulating oogenesis also indicates that the mechanisms that underlie food type-
263 dependent oogenesis onset are not completely the same as those that underlie the food-
264 type differences in total progeny.

265

266 **ASJ neurons modulate food type-dependent oogenesis onset through INS-6**

267 During the larval stages, *ins-6* is expressed in two sensory neurons, ASI and ASJ (***Cornils***
268 ***et al., 2011***). Using the *drcSi68* transcriptional reporter, which expresses *ins-6p::mCherry*
269 in ASI and ASJ, we asked whether the *ins-6* reporter expression changes when the
270 animals are fed OP50 versus CS180. At mid-to-late L3, the stage when the food source
271 can still modulate oogenesis onset (***Figure 3B, Figure 3—supplement 1***), worms grown

272 on CS180 showed higher *ins-6p::mCherry* expression in ASJ, but not in ASI, unlike worms
273 on OP50 (***Figure 6A***). We also found that ASJ-expressed *ins-6*, but not ASI-expressed
274 *ins-6*, is sufficient to rescue the oogenesis onset phenotype of *ins-6* mutants, comparable
275 to the rescue observed when *ins-6* expression is driven from its own promoter (***Figure 6B,***
276 ***Figure 6—supplement 1***). These findings suggest that ASJ modulates early onset of
277 oogenesis by producing INS-6.

278 To confirm that INS-6 does act from ASJ to modulate oogenesis, we next removed
279 the *ins-6* coding sequences from the ASJ neurons, but not from ASI neurons. Loss of *ins-6*
280 from ASJ delayed oogenesis, despite the continued presence of *ins-6* in ASI (***Figure 6C,***
281 ***Figure 6—supplement 1***). Thus, we show that ASJ-expressed *ins-6* is both sufficient and
282 necessary to promote early oogenesis on the CS180 food source.

283

284 **AWA olfactory neurons and insulin receptor signaling regulate food type-**
285 **dependent fertilization rates through different mechanisms**

286 Next, we asked if sensory neurons also influence fertilization. While the *odr-1* mutation
287 had little effect on food type-dependent fertilization rates (***Figure 7—supplement 1***), a
288 mutation in either *osm-3* or another sensory gene, the G protein α subunit *odr-3* (***Roayaie***
289 ***et al., 1998***), suppressed the faster fertilization on CS180 (***Figure 7A and B, Figure 7—***
290 ***supplement 1***). This again suggests a role for sensory neurons in the food type-
291 dependent modulation of fertilization rates.

292 Both *osm-3* and *odr-3* are expressed in several chemosensory neurons, including
293 ADF, ASH, ASI, ASK and ASJ (***Tabish et al., 1995; Roayaie et al., 1998; Taylor et al.,***
294 ***2021***). Ablation of either ADF or ASH had no effect on the food type-induced variation in
295 fertilization rates (***Figure 7C and D, Figure 7—supplement 1***). While the global
296 fertilization rates were lower on OP50 and CS180, loss of either ASI or ASK again did not
297 abolish the food-type differences in fertilization (***Figure 7E and F, Figure 7—supplement***

298 ***1***). In addition, the ASJ neurons, which modulate onset of oogenesis (***Figure 5A and E,***
299 ***Figure 5—supplement 1***), did not affect fertilization rates on OP50 versus CS180 (***Figure***
300 ***7G, Figure 7—supplement 1***), suggesting that ASJ specifically influences oogenesis, but
301 not fertilization. Thus, our data suggest that other neurons expressing either *osm-3* and/or
302 *odr-3*, either individually or in combination, will modulate food type-dependent fertilization.
303 We also asked if the *odr-3*-expressing olfactory neurons AWA, AWB and AWC
304 (***Roayaie et al., 1998***) play a role in this process. While loss of AWB and AWC did not
305 eliminate the fertilization rate differences on OP50 and CS180 (***Figure 7H and I, Figure***
306 ***7—supplement 1***), loss of AWA (***Sengupta et al., 1994; Yoshida et al., 2012***)
307 suppressed the food-type differences in fertilization (***Figure 7J, Figure 7—supplement***
308 ***1***). However, this AWA-dependent regulation of fertilization is independent of the AWA-
309 specific olfactory receptor ODR-10 [***Figure 7—supplement 1***; (***Sengupta et al., 1996***)].
310 This suggests that AWA neurons regulate fertilization in response to food cues that are
311 not ligands of ODR-10.
312 Next, we asked if AWA and ASJ act synergistically during fertilization. However,
313 we found no synergistic effect between the two neurons in regulating this process
314 (compare ***Figure 7G and J to Figure 7K, Figure 7—supplement 1***). To determine if
315 AWA neurons specifically regulate fertilization, we then examined when oogenesis begins
316 in animals lacking AWA. We found that absence of AWA had no effect on early onset of
317 oogenesis on CS180 (***Figure 7L, Figure 7—supplement 1***), similar to its lack of effect on
318 progeny number (***Figure 4A, Figure 4—supplement 1***). Moreover, we observed no
319 synergistic effect between AWA and ASJ in regulating oogenesis onset (***Figure 7L,***
320 ***Figure 7—supplement 1***). Thus, on given diets, we show that there are specific neurons
321 that influence distinct aspects of oocyte development and physiology: ASJ for early
322 oogenesis versus AWA for fertilization.

323 To explore whether AWA regulates fertilization through insulin signaling, we
324 assayed the food type-dependent fertilization rates of insulin signaling mutants. The weak
325 reduction-of-function mutant *daf-2*(*e1368)* or the null *daf-16(mu86)* mutant had little or no
326 significant effect on fertilization (***Figure 8A and C, Figure 8—supplement 1***), but the
327 stronger reduction-of-function mutant *daf-2(e1370)* (***Lin et al., 1997; Gems et al., 1998***)
328 suppressed global fertilization rates (***Figure 8B, Figure 8—supplement 1***). However, the
329 *daf-2(e1370)* mutant fertilization rate on OP50 still differed from that on CS180 (***Figure***
330 ***8B, Figure 8—supplement 1***). This suggests that the DAF-2 receptor modulates overall
331 fertilization rates, but not necessarily in response to food-derived cues. For this reason,
332 the AWA food type-dependent influence on fertilization differs from the effects of insulin
333 receptor signaling on this process.

334 To test if the ILPs that regulate fertilization also differs from the ILPs that regulate
335 total progeny or oogenesis onset, we measured the effects *of ins-6, daf-28* or *ins-1* on
336 fertilization. A single deletion of any of these ILPs had no effect on fertilization rates
337 (***Figure 8D to F, Figure 8—supplement 1***), and deletion mutant combinations of these
338 ILPs (***Figure 8—supplement 1***) did not exhibit any robust phenotypes that mirrored those
339 of the strong *daf-2(e1370)* mutant phenotypes. This implies that there are multiple ILPs
340 that act through the DAF-2 receptor to regulate fertilization. Notably, our findings indicate
341 that the set of ILP activities that regulates fertilization is distinct from the set of ILPs that
342 regulates onset of oogenesis.

343

344 **Discussion**

345 Germline development must be coordinated with existing environmental resources to
346 optmize population survival. The sensory system is an important interface between the
347 environment and an animal's physiology, which suggests a role for the sensory system in
348 germline biology. Not surprisingly, sensory neurons have been implicated in germline

349 proliferation or senescence in *C. elegans* (***Dalfo et al., 2012; Sowa et al., 2015; Aprison***
350 ***and Ruvinsky, 2017***) and potentially in gamete development in mammals (***Boehm et al.,***
351 ***2005; Yoon et al., 2005***). Here we show that distinct sensory neurons acting through
352 insulin-dependent and -independent signaling mechanisms influence specific steps in
353 oocyte development and physiology in response to food-derived cues. Discrete aspects
354 of oocyte biology—oocyte fate determination and successful oocyte fertilization—are thus
355 subject to different sets of cues that are sensed by different cells that work together to
356 control the production of an animal's total progeny.
357

358 **The sensory neurons that regulate oogenesis onset differ from those that affect**
359 **fertilization**

360 Unlike the olfactory neuron AWA, the chemosensory neuron ASJ promotes early onset of
361 oogenesis (***Figure 7L, Figure 7—supplement 1, Figure 9***). This ASJ-dependent effect
362 does not appear to be a general response to stress, like pathogen stress (***Figure 2I,***
363 ***Figure 2—supplement 1***), but a response to specific food cues that are likely not small
364 metabolites (***Figure 2G, Figure 2—supplement 1***). In contrast, the olfactory neuron AWA
365 promotes the increased fertilization rates on the CS180 food source, but not ASJ and the
366 other neurons that we have so far tested (***Figure 7C to K, Figure 7—supplement 1,***
367 ***Figure 9***). Together these data suggest that the sensory cue(s) that promote early
368 oogenesis differ from the sensory cue(s) that affect fertilization.

369 While AWA has a major role in food type-dependent fertilization, it is most likely
370 not the only sensory neuron involved in this process. The *osm-3* mutation, which impairs
371 several sensory neurons (***Tabish et al., 1995***), also partly suppresses the faster
372 fertilization on CS180 (***Figure 7A, Figure 7—supplement 1***). This raises the likelihood
373 that other neurons regulate fertilization. In fact, we find that worms lacking ASI, ASK and
374 AWB neurons fertilize at a slower rate at certain or at all time points on OP50 and CS180,

375 when compared to wild type (***Figure 7E, F and H, Figure 7—supplement 1***). However,
376 these animals still exhibit significant food-type differences in their fertilization rates (***Figure***
377 ***7E, F and H, Figure 7—supplement 1***). This means that ASI, ASK and AWB are not
378 required to regulate food-type effects on fertilization, but might have a role that are
379 independent of food. A mechanism that includes several neurons to regulate fertilization
380 would be expected, since it is a dynamic process that proceeds for several days. This
381 makes it necessary for the worms to sense environmental changes continuously and
382 adjust their reproductive physiology accordingly. Thus, the involvement of multiple sensory
383 neurons would make for a more sensitive and efficient physiology.

384 Interestingly, at least one of the sensory neurons that inhibits germline proliferation
385 (***Aprison and Ruvinsky, 2017***), ASJ, also promotes food type-dependent early oogenesis
386 (this work). This suggests that this sensory neuron might regulate oogenesis onset by
387 regulating the first switch that occurs in the *C. elegans* germline, mitosis (*i.e.*, proliferation)
388 to meiosis (*i.e.*, differentiation) (***Kimble and Crittenden, 2007***). Consistent with this
389 hypothesis, we demonstrate that food type can only modulate onset of oogenesis before
390 the late L3 stage (***Figure 3B, Figure 3—supplement 1***), which coincides with the time
391 before germ cells enter meiosis (***Kimble and Crittenden, 2007***). Thus, some of the
392 sensory neurons that influence the germline might have more than one function at different
393 stages of germ cell development.

394

395 **Oocyte development requires distinct insulin-like signaling mechanisms**

396 Insulin signaling is an important regulator of oogenesis, where impaired signaling leads to
397 reproductive deficits across many species [reviewed by (***Das and Arur, 2017***)]. Here we
398 find that specific ILPs regulate discrete stages of oocyte physiology. The ILP INS-6 acts
399 from the ASJ neuron to modulate food type-dependent early oogenesis (***Figure 6B and***
400 ***C, Figure 6—supplement 1, Figure 9***), whereas it appears to have little or no effect on

401 oocyte fertilization rates (***Figure 8D, Figure 8—supplement 1***). Although insulin receptor
402 DAF-2 signaling does not appear to mediate the AWA neuron-dependent food-type effects
403 on fertilization, DAF-2 does regulate overall fertilization independent of food sources
404 (***Figure 8B, Figure 8—supplement 1, Figure 9***), where its ILP ligands remain to be
405 identified. Since fertilization depends on oocyte maturation (***McCarter et al., 1999***), our
406 data also suggest that different ILPs regulate specific stages of oogenesis—onset versus
407 maturation.

408 Our findings further suggest that at least one of these ILPs, INS-6, can act
409 independent of DAF-16, a known transcriptional effector of the DAF-2 receptor (***Figure***
410 ***5F, Figure 5—supplement 1***). Distinct insulin-like signaling mechanisms—*daf-16*-
411 independent and *daf-16*-dependent—might be necessary for optimal oogenesis and
412 fertilization. A worm's number of progeny will likely be impacted by the timing of the
413 spermatogenesis-to-oogenesis switch, as well as by successful fertilization. Hence,
414 distinct ILP signaling mechanisms that can respond to disparate environmental cues might
415 also explain the variability in the number of progeny of *daf-16* mutants (***Figure 4B and E,***
416 ***Figure 4—supplement 1***).

417 ILPs might encode and integrate diverse cues that influence oocyte development.
418 Considering the pleiotropic effects of insulin signaling on metazoan reproduction (***Das and***
419 ***Arur, 2017***), it is possible that the multiple ILPs present in other animals (***Allen et al.,***
420 ***2015***) will also have specific roles in coordinating oogenesis with fluctuations in a given
421 environment. Thus, our study suggests that successful fertilization will require the careful
422 integration of multiple environmental inputs through ILPs acting on the germline from
423 neuronal, and potentially non-neuronal, cells.

424

425 **Materials and Methods**

426 **Worm strains and culture**

427 *General maintenance. C. elegans* were cultured on NGM agar plates (***Brenner, 1974***)
428 seeded with *E. coli* OP50, CS180, CS2429, or HT115 or with *S. marcescens* strains. All
429 bacterial strains were initially cultured in Luria broth (LB) medium to logarithmic phase,
430 prior to seeding the NGM agar plates. All animals were well-fed for at least two generations
431 before any phenotypic analyses were conducted. All experiments were performed at 25°C,
432 except for those that included the *daf-2(e1368)* or *daf-2(e1370)* temperature-sensitive
433 mutations. *daf-2* mutants grown as eggs until the L1 stage at 25°C become
434 developmentally arrested (***Gems et al., 1998***). Thus, these mutants were first grown at
435 20°C, the permissive temperature, and shifted to 25°C before the critical periods defined
436 for food-dependent modulation of oogenesis onset or fertilization, along with their
437 corresponding controls. See ***Supplementary File 1*** for the list of genotypes of the strains
438 used in this study, which include the neuronally ablated animals. All strains generated in
439 this study are available upon request.

440 *Generation of the lin-41::GFP daf-16(mu86) recombinant.* To recombine
441 *lin-41::GFP* with the *daf-16(mu86)* deletion on chromosome I, the strain carrying
442 *lin-41(tn1541[GFP::tev::s::lin-41])* (***Spike et al., 2014***) was crossed to a *daf-16(mu86)*
443 homozygote. Among the subsequent progeny of the *lin-41::GFP* + / + *daf-16* cross-
444 progeny, we identified 1 recombination event out of 50 chromosomes, which was
445 homozygous for *lin-41::GFP* and heterozygous for *daf-16(mu86)*. This animal was allowed
446 to reproduce to isolate the homozygous *lin-41::GFP daf-16(mu86)* recombinant strain.

447 *Generation of the loxP-flanked ins-6 strain, syb7547.* A region of the *ins-6* genomic
448 locus, which begins at the translation start codon in exon 1 until the translation stop codon
449 in exon 2, was replaced with the *ins-6* open reading frame (ORF) through CRISPR/Cas9
450 technology by SunyBiotech (Fujian, China). The inserted ORF, which lacks intron 1, was
451 flanked at both ends with the *loxP* sequence, 5'-ATA ACT TCG TAT AGC ATA CAT TAT
452 ACG AAG TTA T-3'. The first *loxP* sequence was inserted 3 bases upstream of the start

453 codon, whereas the second *loxP* sequence was inserted immediately after the stop codon.
454 Two synonymous nucleotide changes were introduced into the inserted ORF to prevent
455 its cleavage by Cas9 during the integration step: L14L (CTC to CTG) and C96C (TGC to
456 TGT). *syb7547* was outcrossed four times to the *lin-41(tn1541[GFP::tev::s::lin-41])* strain
457 (***Spike et al., 2014***) before analysis in the presence or absence of the *trx-1p::nCRE*
458 recombinase transgene (ASJp::*CRE*). Like animals that have a wild-type *ins-6* genomic
459 locus, *ins-6(syb7547)* animals showed an earlier onset of oogenesis on CS180 during
460 mid-L4 (***Figure 6C, Figure 6—supplement 1***) in the absence of the *trx-1p::nCRE*
461 recombinase.

462 *Generation of the ASJp::CRE recombinase strain.* We_drove CRE recombinase
463 (gift of Mario de Bono) from the *trx-1* promoter (***Miranda-Vizuete et al., 2006; Cornils et***
464 ***al., 2011***), with an *unc-54* 3' UTR from pPD95.77 (gift of Andrew Fire; pQZ116). The
465 plasmid pQZ116, was introduced into a *lin-41(tn1541[GFP::tev::s::lin-41])*; *ins-6(tm2416)*
466 animal, as an extrachromosomal array.

467

468 **Measurement of the rate of development**

469 L1 larvae that hatched within a 2-hr period on each bacterial food source were collected
470 and allowed to grow at 25°C for 32 hrs on the same food source. The number of animals
471 that were L1, L2, L3 or L4 larvae or adults were counted and represented as a percentage
472 of the total population. The chi-square test was used to compare the stage distributions of
473 worms fed the different bacteria.

474

475 **Measurement of sperm and arrested oocytes**

476 To count the number of sperm, 2- to 3-hr-old adult OD95 hermaphrodites that carry the
477 transgene *pie-1p::mCherry::his-58* (***McNally et al., 2006***) were anesthetized on a 1%
478 agarose pad that contained 6 mM sodium azide. Series of Z-stack images of the

479 spermathecae were captured at 100 msec as the exposure time, using a Nikon Eclipse
480 Ti-E microscope and a Photometrics Coolsnap Myo cooled digital camera. The number of
481 sperm were counted as red fluorescent puncta across the entire stacks.

482 To measure the number of arrested oocytes, young wild-type adult hermaphrodites
483 were anesthetized as described above. The gonads were imaged under differential
484 interference contrast microscopy. Counts from only one gonad arm were reported per
485 animal. The Student's t-test was used to compare gamete counts between animals.

486

487 **Measurement of total progeny**

488 Individual young adult hermaphrodites were grown on a 35-mm plate seeded with the
489 indicated bacteria. The mother was transferred to a new plate every 12-24 hrs until
490 reproduction ceased entirely. Total progeny that hatched were counted and reported. At
491 least ten animals were tested in each trial, and each strain studied was assayed in multiple
492 independent trials. To analyze the *daf-2* mutants and their corresponding controls, worms
493 were first grown at 20°C, before they were transferred to 25°C at the early L3 stage.
494 Statistical comparisons across multiple groups were determined by one-way ANOVA,
495 followed by Tukey's correction.

496

497 **Imaging the oogenesis reporters**

498 Control and mutants carrying *lin-41::GFP* (***Spike et al., 2014***) or *oma-1::GFP* (***Lin, 2003***)
499 were imaged in parallel at 400X magnification, using a Nikon Eclipse Ti-E microscope and
500 a Photometrics Coolsnap Myo cooled digital camera or a Nikon Eclipse Ni-U microscope
501 and a Photometrics Coolsnap ES2 cooled digital camera. The exposure time was set at
502 500 msec, and the presence or absence of GFP was reported at different stages. The
503 stages of the animal were determined by observing the vulval morphology under 400x, as
504 described by (***Mok et al., 2015***), and illustrated in ***Figure 1F***. Based on the substages

505 described by Mok et al. (2015), early L4 corresponded to the L4.0 to L4.2 substages; mid
506 L4, to the L4.3 to L4.5 substages; late L4, to the L4.6 to L4.8 substages, when the finger-
507 like structures that formed at the sides of the vulva (red arrowheads in ***Figure 1F***) had
508 started to migrate ventrally; and lethargus to the L4.9 substage. To analyze the *daf-2*
509 mutants and their corresponding controls, worms were grown at 20°C and transferred to
510 25°C at the early L3 stage and then imaged at different subsequent stages. Statistical
511 comparisons across multiple groups used the Fisher's exact test.
512

513 **Imaging the *ins-6p::mCherry* transcriptional reporter**

514 *Generation of the ins-6p::mCherry transcriptional reporter.* The mCherry gene was flanked
515 with 1.64-kb sequences upstream of the *ins-6* start codon and 7.57-kb sequences
516 downstream of the *ins-6* stop codon. This reporter was cloned into a MosSCI vector for
517 integration (pQL147) at the ttTi5605 site of chromosome II (***Frøkjær-Jensen et al., 2008***)
518 to generate the *ins-6p::mCherry drcSi68* worms.

519 *Imaging of drcSi68 worms.* The worms were grown continuously on OP50 or
520 CS180. Worms at the mid-to-late L3 stage were imaged at 1000x magnification, using a
521 Nikon Eclipse Ni-U microscope and a Photometrics Coolsnap ES2 cooled digital camera.
522 The exposure time was set at 50 msec. Fluorescence intensities were quantified using a
523 built-in fluorescence quantification algorithm (NIS-Elements, Nikon Instruments, Inc).
524 Statistical analyses used two-way ANOVA and Tukey's correction.
525

526 **Measuring the rates of fertilization**

527 For every trial, ten to twelve young adult worms were grown singly for a specified number
528 of hours. At the end of each time point, the mother was bleached in a 5% sodium
529 hypochlorite solution to release and count the fertilized embryos within its uterus. We also
530 counted the number of hatched progeny that were laid on the plates. The total number of

531 oocytes fertilized at each time point was the sum of the embryos within the uterus and
532 those laid on the plates. We then divided the total number of fertilized oocytes by the
533 duration of the collection to calculate the rate of fertilization at that specific time point. To
534 analyze the *daf-2* mutants and their corresponding controls, worms were first grown at
535 20°C and transferred to 25°C at the early L4 stage. Statistical comparisons across multiple
536 groups were performed by two-way ANOVA and Tukey's correction.

537 To compare the food type-dependent changes in fertilization rates between wild
538 type and different groups of animals, we normalized the 12- to 24-hour fertilization rates
539 on CS180 to the 12- to 24-hour fertilization rates on OP50 of a given strain. The resulting
540 normalized means were then compared to the food type-dependent change in fertilization
541 rates of wild-type controls. Thus, p values were calculated by obtaining the t-score after
542 comparing the percent change in wild type on CS180 versus OP50 to the percent change
543 for the specific mutant on CS180 versus OP50.

544

545 **Food-switch experiments**

546 *C. elegans* were grown on each bacteria and then transferred to the second bacteria at
547 different stages. The early L3, late L3, early L4, and late L4 were determined based on
548 the developmental rates of the animals on OP50 and CS180. L1 larvae that hatched within
549 a 1-hr period at 25°C were collected and allowed to develop further at this temperature on
550 the first bacteria for a certain duration before being shifted to the second bacteria: 20 hrs
551 for early L3, 24 hrs for late L3, and 26 and 30 hrs, respectively, for early and late L4. The
552 early and late L4 stages were also confirmed by examining vulval morphology. To
553 minimize contamination from the earlier bacteria, worms were allowed to roam on the
554 second bacteria for 45-60 minutes and then transferred to a fresh plate seeded with the
555 second bacteria. After this transfer, worms were assayed for total number of progeny,
556 fertilization rate, or the expression of the *lin-41::GFP* oogenesis reporter.

557 To compare the food type-dependent changes in fertilization rates during the food
558 switches, we normalized the 12- to 24-hour fertilization rates of the CS180-to-OP50
559 switched animals to the 12- to 24-hour fertilization rates of the OP50-to-CS180 switched
560 animals. The p values of the subsequent normalized means were calculated by obtaining
561 the t-score after comparing the percent change in food-switched animals to the percent
562 change in non-switched controls on CS180.
563

564 **Preparation of CS180-conditioned media for supplementation experiments**

565 For each experimental trial, we grew a single colony of *E. coli* CS180 in 10 to 25 ml LB to
566 an optical density of 0.5 to 0.6 at 600 nm (logarithmic growth phase) at 37ºC. We then
567 centrifuged 3 to 4 ml of the CS180 culture at 2380 x g at 4ºC for 15 min to remove the
568 bacterial pellet and isolate the CS180-conditioned medium. We added 100 μl of the
569 CS180-conditioned medium to each lawn of *E. coli* OP50 on 35-mm NGM agar plates to
570 determine the effects of the medium on oogenesis onset and oocyte fertilization rates.

571 In addition, we passaged the CS180-conditioned medium through a sterile nylon
572 membrane syringe filter with a 0.45 μm-diameter pore size. We added 100 μl of the
573 collected filtrate to a different lawn of OP50 on a 35-mm NGM agar plate to test whether
574 the CS180-derived cue(s) that modulate oocyte physiology are small, free metabolites. To
575 verify that the potential loss of CS180 cue(s) was not due to the cue(s) adsorbing to the
576 membrane, we pre-incubated 3 to 4 ml of the CS180-conditioned medium with a postage
577 stamp-sized 0.45 μm-diameter nylon membrane. The pre-incubation was carried out for
578 10 min at room temperature using a nutator set at low speed. We also added 100 μl of the
579 pre-adsorbed medium to other lawns of OP50 on 35-mm NGM agar plates. Preadsorption
580 of the CS180-conditioned media with a nylon membrane filter still led to faster fertilization,
581 similar to CS180-fed controls (***Figure 2—supplement 1***).

582

583 **Statistical analysis**

584 Statistical analyses were done using GraphPad Prism 8 software. For more details, refer
585 to above and the legends of the figures and their supplements.

586

587 **Acknowledgements**

588 We thank S. Mitani, the *Caenorhabditis* Genetics Center (funded by NIH P40 OD010440),
589 J. Apfeld, T. Chen, M. de Bono, D. Ferkey, A. Fire, M. Goodman, J. Klena, and P.
590 Sengupta for strains used in this study. We also thank S. Kuchin of University of
591 Wisconsin-Milwaukee for generously assisting us in the statistical analyses of total
592 fertilization rates of different worm genotypes on different food sources (***Figures 3, 7 and***
593 ***8 Supplements, sheets on normalized fertilization rates***). We further thank A. Shevade
594 and M. Salsaa for comments on the manuscript. This work was supported by a Wayne
595 State University Graduate Research Assistantship to S. M., an ERC Starting Investigator
596 Grant (NeuroAge 242666) and a Research Councils UK Fellowship to Q. C., and by
597 Wayne State University, the Alcedo family and NIH (R01 GM108962) to J. A.

598 **References**

599

600 Allen E, Ren J, Zhang Y and Alcedo J. 2015. Sensory systems: their impact on *C.*
601 *elegans* survival, *Neuroscience* **296**: 15-25.
602 Aprison EZ and Ruvinsky I. 2017. Counteracting ascarosides act through distinct
603 neurons to determine the sexual identity of *C. elegans* pheromones, *Curr Biol* **27**: 2589-
604 2599.
605 Barton MK and Kimble J. 1990. *fog-1*, a regulatory gene required for specification of
606 spermatogenesis in the germ line of *Caenorhabditis elegans*, *Genetics* **125**: 29-39.
607 Boehm U, Zou Z and Buck LB. 2005. Feedback loops link odor and pheromone signaling
608 with reproduction, *Cell* **123**: 683-95.
609 Brenner S. 1974. The genetics of *Caenorhabditis elegans*, *Genetics* **77**: 71-94.
610 Chen Z, Hendricks M, Cornils A, Maier W, Alcedo J and Zhang Y. 2013. Two insulin-like
611 peptides antagonistically regulate aversive olfactory learning in *C. elegans*, *Neuron* **77**:
612 572-85.
613 Cornils A, Gloeck M, Chen Z, Zhang Y and Alcedo J. 2011. Specific insulin-like peptides
614 encode sensory information to regulate distinct developmental processes, *Development*
615 **138**: 1183-93.
616 Dalfo D, Michaelson D and Hubbard EJ. 2012. Sensory regulation of the *C. elegans*
617 germline through TGF-beta-dependent signaling in the niche, *Curr Biol* **22**: 712-9.
618 Das D and Arur S. 2017. Conserved insulin signaling in the regulation of oocyte growth,
619 development, and maturation, *Mol Reprod Dev* **84**: 444-459.
620 Dasgupta S, Fernandez L, Kameyama L, Inada T, Nakamura Y, Pappas A and Court
621 DL. 1998. Genetic uncoupling of the dsRNA-binding and RNA cleavage activities of the
622 *Escherichia coli* endoribonuclease III - the effect of dsRNA binding on gene expression,
623 *Mol Microbiol* **28**: 629–640.

624 Detwiler MR, Reuben M, Li X, Rogers E and Lin R. 2001. Two zinc finger proteins, OMA-
625 1 and OMA-2, are redundantly required for oocyte maturation in *C. elegans*, *Dev Cell* **1**:
626 187-199.
627 Duret L, Guex N, Peitsch MC and Bairoch A. 1998. New insulin-like proteins with
628 atypical disulfide bond pattern characterized in *Caenorhabditis elegans* by comparative
629 sequence analysis and homology modeling, *Genome Res* **8**: 348-53.
630 Fernandes de Abreu DA, Caballero A, Fardel P, Stroustrup N, Chen Z, Lee K, Keyes
631 WD, Nash ZM, Lopez-Moyado IF, Vaggi F et al. 2014. An insulin-to-insulin regulatory
632 network orchestrates phenotypic specificity in development and physiology, *PLoS Genet*
633 **10**: e1004225.
634 Frøkjær-Jensen C, Wayne Davis M, Hopkins CE, Newman BJ, Thummel JM, Olesen S-
635 P, Grunnet M and Jorgensen EM. 2008. Single-copy insertion of transgenes in
636 *Caenorhabditis elegans*, *Nat Genet* **40**: 1375-1383.
637 Gems D, Sutton AJ, Sundermeyer ML, Albert PS, King KV, Edgley ML, Larsen PL and
638 Riddle DL. 1998. Two pleiotropic classes of *daf-2* mutation affect larval arrest, adult
639 behavior, reproduction and longevity in *Caenorhabditis elegans*, *Genetics* **150**: 129-55.
640 Greenstein D (2005) Control of oocyte meiotic maturation and fertilization. in The C.
641 elegans Research Community (ed.) *WormBook*: WormBook.
642 Hasegawa H, Naganuma K, Nakagawa Y and Matsuyama T. 2003. Membrane filter
643 (pore size, 0.22–0.45 μm; thickness, 150 μm) passing-through activity of *Pseudomonas*
644 *aeruginosa* and other bacterial species with indigenous infiltration ability, *FEMS*
645 *Microbiol Lett* **223**: 41-46.
646 Kawano T, Ito Y, Ishiguro M, Takuwa K, Nakajima T and Kimura Y. 2000. Molecular
647 cloning and characterization of a new insulin/IGF-like peptide of the nematode
648 *Caenorhabditis elegans*, *Biochem Biophys Res Commun* **273**: 431-6.

649 Kimble J and Crittenden SL. 2007. Controls of germline stem cells, entry into meiosis,
650 and the sperm/oocyte decision in *Caenorhabditis elegans*, *Annu Rev Cell Dev Biol* **23**:
651 405-433.
652 Kimura KD, Tissenbaum HA, Liu Y and Ruvkun G. 1997. *daf-2*, an insulin receptor-like
653 gene that regulates longevity and diapause in *Caenorhabditis elegans*, *Science* **277**:
654 942-6.
655 Kodama E, Kuhara A, Mohri-Shiomi A, Kimura KD, Okumura M, Tomioka M, Iino Y and
656 Mori I. 2006. Insulin-like signaling and the neural circuit for integrative behavior in *C.*
657 *elegans*, *Genes Dev* **20**: 2955–2960.
658 L'Etoile ND and Bargmann CI. 2000. Olfaction and odor discrimination are mediated by
659 the *C. elegans* guanylyl cyclase ODR-1, *Neuron* **25**: 575-86.
660 Li W, Kennedy SG and Ruvkun G. 2003. *daf-28* encodes a *C. elegans* insulin
661 superfamily member that is regulated by environmental cues and acts in the DAF-2
662 signaling pathway, *Genes Dev* **17**: 844-58.
663 Lin K, Dorman JB, Rodan A and Kenyon C. 1997. *daf-16*: An HNF-3/forkhead family
664 member that can function to double the life-span of *Caenorhabditis elegans*, *Science*
665 **278**: 1319–1322.
666 Lin R. 2003. A gain-of-function mutation in oma-1, a C. elegans gene required for oocyte
667 maturation, results in delayed degradation of maternal proteins and embryonic lethality,
668 *Dev Biol* **258**: 226-239.
669 Lopez Andrew L, III, Chen J, Joo H-J, Drake M, Shidate M, Kseib C and Arur S. 2013.
670 DAF-2 and ERK couple nutrient availability to meiotic progression during *Caenorhabditis*
671 *elegans* oogenesis, *Dev Cell* **27**: 227-240.
672 Maier W, Adilov B, Regenass M and Alcedo J. 2010. A neuromedin U receptor acts with
673 the sensory system to modulate food type-dependent effects on *C. elegans* lifespan,
674 *PLoS Biol* **8**: e1000376.

675 McCarter J, Bartlett B, Dang T and Schedl T. 1999. On the control of oocyte meiotic
676 maturation and ovulation in *Caenorhabditis elegans*, *Dev Biol* **205**: 111-28.
677 McNally K, Audhya A, Oegema K and McNally FJ. 2006. Katanin controls mitotic and
678 meiotic spindle length, *J Cell Biol* **175**: 881-891.
679 Michaelson D, Korta DZ, Capua Y and Hubbard EJ. 2010. Insulin signaling promotes
680 germline proliferation in *C. elegans*, *Development* **137**: 671-80.
681 Miller MA, Nguyen VQ, Lee MH, Kosinski M, Schedl T, Caprioli RM and Greenstein D.
682 2001. A sperm cytoskeletal protein that signals oocyte meiotic maturation and ovulation,
683 *Science* **291**: 2144-7.
684 Miranda-Vizuete A, Gonzalez JC, Gahmon G, Burghoorn J, Navas P and Swoboda P.
685 2006. Lifespan decrease in a Caenorhabditis elegans mutant lacking TRX-1, a
686 thioredoxin expressed in ASJ sensory neurons, *FEBS Lett* **580**: 484-90.
687 Mok DZ, Sternberg PW and Inoue T. 2015. Morphologically defined sub-stages of *C.*
688 *elegans* vulval development in the fourth larval stage, *BMC Dev Biol* **15**: 26.
689 Murphy CT and Hu PJ. 2013. Insulin/insulin-like growth factor signaling in C. elegans,
690 *WormBook*: 1-43.
691 Noble DC, Aoki ST, Ortiz MA, Kim KW, Verheyden JM and Kimble J. 2016. Genomic
692 analyses of sperm fate regulator targets reveal a common set of oogenic mRNAs in
693 *Caenorhabditis elegans*, *Genetics* **202**: 221-34.
694 Ogg S, Paradis S, Gottlieb S, Patterson GI, Lee L, Tissenbaum HA and Ruvkun G.
695 1997. The Fork head transcription factor DAF-16 transduces insulin-like metabolic and
696 longevity signals in *C. elegans*, *Nature* **389**: 994-9.
697 Perez MF, Shamalnasab M, Mata-Cabana A, Della Valle S, Olmedo M, Francesconi M
698 and Lehner B. 2021. Neuronal perception of the social environment generates an
699 inherited memory that controls the development and generation time of *C. elegans*, *Curr*
700 *Biol* **31**: 1 - 13.

701 Pierce SB, Costa M, Wisotzkey R, Devadhar S, Homburger SA, Buchman AR, Ferguson
702 KC, Heller J, Platt DM, Pasquinelli AA et al. 2001. Regulation of DAF-2 receptor
703 signaling by human insulin and *ins-1*, a member of the unusually large and diverse *C.*
704 *elegans* insulin gene family, *Genes Dev* **15**: 672-86.
705 Pradel E, Parker CT and Schnaitman CA. 1992. Structures of the rfaB, rfaI, rfaJ, and
706 rfaS genes of Escherichia coli K-12 and their roles in assembly of the lipopolysaccharide
707 core, *J Bacteriol* **174**: 4736-45.
708 Pradel E, Zhang Y, Pujol N, Matsuyama T, Bargmann CI and Ewbank JJ. 2007.
709 Detection and avoidance of a natural product from the pathogenic bacterium *Serratia*
710 *marcescens* by *Caenorhabditis elegans*, *Proc Natl Acad Sci USA* **104**: 2295-2300.
711 Ritter AD, Shen Y, Fuxman Bass J, Jeyaraj S, Deplancke B, Mukhopadhyay A, Xu J,
712 Driscoll M, Tissenbaum HA and Walhout AJM. 2013. Complex expression dynamics and
713 robustness in *C. elegans* insulin networks, *Genome Research* **23**: 954-965.
714 Roayaie K, Crump JG, Sagasti A and Bargmann CI. 1998. The G alpha protein ODR-3
715 mediates olfactory and nociceptive function and controls cilium morphogenesis in *C.*
716 *elegans* olfactory neurons, *Neuron* **20**: 55-67.
717 Sengupta P, Chou JH and Bargmann CI. 1996. *odr-10* encodes a seven transmembrane
718 domain olfactory receptor required for responses to the odorant diacetyl, *Cell* **84**: 899-
719 909.
720 Sengupta P, Colbert HA and Bargmann CI. 1994. The *C. elegans* gene *odr-7* encodes
721 an olfactory-specific member of the nuclear receptor superfamily, *Cell* **79**: 971-80.
722 Sowa JN, Mutlu AS, Xia F and Wang MC. 2015. Olfaction modulates reproductive
723 plasticity through neuroendocrine signaling in *Caenorhabditis elegans*, *Curr Biol* **25**:
724 2284-9.
725 Spike CA, Coetzee D, Eichten C, Wang X, Hansen D and Greenstein D. 2014. The
726 TRIM-NHL protein LIN-41 and the OMA RNA-binding proteins antagonistically control

727 the prophase-to-metaphase transition and growth of *Caenorhabditis elegans* oocytes,
728 *Genetics* **198**: 1535-58.
729 Tabish M, Siddiqui ZK, Nishikawa K and Siddiqui SS. 1995. Exclusive expression of *C.*
730 *elegans osm-3* kinesin gene in chemosensory neurons open to the external
731 environment, *J Mol Biol* **247**: 377-89.
732 Takiff HE, Chen S-M and Court DL. 1989. Genetic analysis of the *rnc* operon of
733 *Escherichia coli*, *J Bacteriol* **171**: 2581–2590.
734 Taylor SR, Santpere G, Weinreb A, Barrett A, Reilly MB, Xu C, Varol E, Oikonomou P,
735 Glenwinkel L, McWhirter R et al. 2021. Molecular topography of an entire nervous
736 system, *Cell* **184**: 4329-4347.e23.
737 Tomioka M, Adachi T, Suzuki H, Kunitomo H, Schafer WR and Iino Y. 2006. The
738 insulin/PI 3-kinase pathway regulates salt chemotaxis learning in *Caenorhabditis*
739 *elegans*, *Neuron* **51**: 613-25.
740 Ward S and Carrel JS. 1979. Fertilization and sperm competition in the nematode
741 *Caenorhabditis elegans*, *Dev Biol* **73**: 304-21.
742 Yoon H, Enquist LW and Dulac C. 2005. Olfactory inputs to hypothalamic neurons
743 controlling reproduction and fertility, *Cell* **123**: 669-82.
744 Yoshida K, Hirotsu T, Tagawa T, Oda S, Wakabayashi T, Iino Y and Ishihara T. 2012.
745 Odour concentration-dependent olfactory preference change in *C. elegans*, *Nat*
746 *Commun* **3**: 739.
747 Zhang P, Snyder S, Feng P, Azadi P, Zhang S, Bulgheresi S, Sanderson KE, He J,
748 Klena J and Chen T. 2006. Role of N-acetylglucosamine within core lipopolysaccharide
749 of several species of gram-negative bacteria in targeting the DC-SIGN (CD209), *J*
750 *Immunol* **177**: 4002-11.

751

752 **Figure 1. *C. elegans* exhibit early oogenesis and faster fertilization rate in response**
753 **to a specific bacterial food source. (A)** The *C. elegans* reproductive developmental
754 program, which depicts the timing of the spermatogenesis-to-oogenesis switch at L4. **(B)**
755 Somatic development was unchanged between animals fed the two *E. coli* food types (n
756 = 286 on OP50; n = 265 on CS180; p = 0.72). **(C-E)** Worms fed OP50 had more progeny
757 (**C**), slower fertilization rates **(D)**, and more sperm **(E)** than worms fed CS180. **(F)**
758 Simplified illustration of vulval morphology at various sub-stages of L4, where the nuclei
759 of specific cells are shown [adapted from (***Mok et al., 2015***)]. Red arrowheads indicate
760 the finger-like structures at the sides of the vulva, which migrate ventrally during late L4.
761 Lethargus is the molting period from L4 to young adulthood. **(G)** Early onset of oogenesis
762 was determined by the initial expression of *lin-41::GFP*. Anterior is to the left and dorsal is
763 to the top of each panel. Scale bar is 10 μm. **(H-I)** Worms on CS180 began oogenesis
764 earlier at mid L4 than worms on OP50, based on the earliest *lin-41::GFP* **(H)** or
765 *oma-1::GFP* **(I)** expression. Early oogenesis onset at mid L4 is highlighted by a dotted box
766 in these panels and later panels. **(J)** Adults on CS180 had more arrested oocytes than
767 age-matched adults on OP50. Error bars in **(C-D)** represent standard deviation; **(E**, **J**),
768 SEM. ** indicates $p \leq 0.01$; and ***, $p \leq 0.001$.

769 **Figure 1—supplement 1. Statistical analyses of wild-type progeny,**
770 **fertilization rates and oogenesis onset on OP50 versus CS180.** Sheet 1 shows the
771 analyses for total progeny; sheet 2, for fertilization rates; and sheet 3, for onset of
772 oogenesis. On sheets 1 and 2, N is the total number of animals assayed. Means are from
773 pooled data from multiple, independent trials. SD is the standard deviation. On sheet 3,
774 GFP (+) and GFP (-) are animals that expressed or did not express the indicated
775 oogenesis markers, respectively. On all sheets, significant p values are shown in red and
776 italicized. The **Figure 1** panels associated with the data are indicated. WT denotes wild
777 type. * denotes p values between OP50-fed worms versus CS180-fed worms.

778 **Figure 2. The CS180 effects on oogenesis are independent of LPS length and absent**
779 **in HT115 and other bacteria. (A)** The LPS of *E. coli* B and K-12 strains. CS2429 is
780 derived from CS180 and has a truncated LPS (***Maier et al., 2010***, and references therein).
781 The dotted blue line indicates the site of truncation. **(B-D)** The shorter LPS of CS2429
782 elicited the same total progeny **(B)**, a similar pattern of oogenesis reporter expression **(C)**,
783 and the same rate of fertilization **(D)**, as the longer LPS of the parent strain CS180. **(E-F)**
784 *C. elegans* oogenesis onset **(E)** and fertilization rates **(F)** on the *E. coli* K-12 HT115
785 bacteria were compared to those of *C. elegans* on OP50 and CS180. **(G-H)** Oogenesis at
786 mid L4 **(G)** and fertilization rates at 22 hr **(H)** on OP50 and CS180 were compared to
787 oogenesis onset **(G)** and fertilization rates **(H)** on OP50 that had been supplemented with:
788 (i) CS180-conditioned LB media (med) or (ii) CS180-conditioned media that was filtered
789 through a 0.45-μm nylon membrane (filtrate). For comparison, worms on OP50 that had
790 been supplemented with LB alone or with LB that was filtered through a nylon membrane
791 are also shown. **(I)** Two strains of the pathogen *Serratia marcescens*, Db1140 and Db11,
792 did not induce early oogenesis. Error bars represent standard deviations. * indicates $p \leq$
793 0.05; **, $p \leq 0.01$; ***, $p \leq 0.001$; and suppl, supplementation.

794 **Figure 2—supplement 1. Statistical analyses of wild-type progeny,**
795 **oogenesis onset and fertilization rates on OP50, LPS mutant bacteria, HT115,**
796 ***Serratia marcescens* and CS180-conditioned media.** Sheet 1 shows the analyses for
797 total progeny; sheet 2, for onset of oogenesis; and sheet 3, for fertilization rates. On sheets
798 1 and 3, N is the total number of animals that were assayed. Means are from pooled data
799 from multiple, independent trials. SD is the standard deviation. On sheet 2, GFP (+) and
800 GFP (-) are animals that expressed or did not express the *lin-41::GFP* oogenesis marker,
801 respectively. On all sheets, significant p values are shown in red and italicized. The **Figure**
802 **2** panels associated with the data are indicated. WT denotes wild type. NA means not
803 applicable.

804 **Figure 3. Food type modulates oogenesis onset during L3 and fertilization rates**
805 **after early L4.** Wild-type *C. elegans* were shifted between *E. coli* OP50 and CS180 at
806 different stages of larval development. **(A-B)** The critical period for food-type modulation
807 of total progeny **(A)** and oogenesis onset **(B)** is around late L3. **(C-F)** The critical period
808 for modulation of fertilization is after early L4. Error bars represent standard deviations. *
809 indicates $p \leq 0.05$; **, $p \leq 0.01$; ***, $p \leq 0.001$; ns, not significant; and leth, lethargus.

810 **Figure 3—supplement 1. Statistical analyses of the progeny, oogenesis**
811 **onset and fertilization rates in food-switched versus non-switched wild-type**
812 **animals.** Sheet 1 shows the analyses for total progeny; sheet 2, for onset of oogenesis;
813 sheet 3, for fertilization rates before normalization; and sheet 4, for normalized fertilization
814 rates. On sheets 1 and 3, N is the total number of animals that were assayed. Means are
815 from pooled data from multiple, independent trials. SD is the standard deviation. On sheet
816 2, GFP (+) and GFP (-) are animals that expressed or did not express the *lin-41::GFP*
817 oogenesis marker, respectively. On all sheets, significant p values are shown in red and
818 italicized. The **Figure 3** panels associated with the data are indicated. Symbols,
819 abbreviations and superscripted letters are described within each sheet.

820 **Figure 4. The ASJ sensory neuron and insulin-like peptide INS-6 alter total progeny**
821 **in response to food type**. **(A)** Food-type differences in total progeny were lost in sensory
822 mutants *osm-3* and *odr-1* and in animals lacking the ASJ neurons. **(B)** Total progeny of
823 the strong reduction-of-function mutant *daf-2(e1370)* and the *daf-16* loss-of-function
824 mutant on OP50 and CS180. **(C-D)** OP50- and CS180-dependent progeny of ILP deletion
825 mutants, *daf-28(tm2308)* and *ins-1(nr2091)* **(C)** and *ins-6(tm2416)* **(D)**. **(E)** Epistasis
826 analysis between the food type-dependent total progeny phenotypes of *daf-16(mu86)* and
827 *ins-6(tm2416)*. While the animals in **(A)** and **(C-E)** were grown continuously at 25°C, the
828 animals in **(B)** were shifted from 20°C to 25°C at the early L3 stage, because *daf-2* mutants
829 arrest developmentally prior to the L3 stage at 25°C but not at 20°C. Error bars represent
830 standard deviations. ** indicates $p \leq 0.01$; ***, $p \leq 0.001$; and ns, not significant.

831 **Figure 4—supplement 1. Statistical analyses of total progeny of different**
832 **groups of animals on OP50 versus CS180.** N is the total number of mothers that were
833 assayed. Means are from pooled data from multiple, independent trials. SD is the standard
834 deviation. Significant p values are shown in red and italicized. The **Figure 4** panels
835 associated with the data are indicated. * denotes p values between OP50-fed worms
836 versus CS180-fed worms. # denotes experiments in which animals that carry the
837 *daf-2(e1368)*, *daf-2(e1370)*, or *daf-16(mu86)* mutation and the corresponding wild-type
838 controls were grown at 20°C and transferred to 25°C at the early L3 stage. All other
839 experiments involved animals that were continuously grown at 25°C.

840 **Figure 5. ASJ neurons and *ins-6* promote early oogenesis onset. (A)** Food type-
841 dependent expression of the oogenesis reporter *lin-41::GFP* in control and different
842 sensory mutants. **(B-D)** *lin-41::GFP* expression in *daf-2* reduction-of-function mutants **(B),**
843 *daf-16(mu86)* **(C)** and in ILP deletion (Δ) mutants **(D)**. **(E)** Food type-dependent expression
844 of a second oogenesis reporter, *oma-1::GFP*, in control, ASJ-ablated and *ins-6(tm2416)*
845 worms. **(F)** Loss of *daf-16* did not rescue the delay in oogenesis onset in *ins-6(tm2416)*
846 mutants. Controls and *daf-2* mutants in **(B)** were shifted from 20°C to 25°C as early L3s.
847 In contrast, all other animals were continuously grown at 25°C on OP50 (white bars) or
848 CS180 (grey bars). * indicates $p \leq 0.05$; **, $p \leq 0.01$; ***, $p \leq 0.001$; and leth, lethargus.

849 **Figure 5—supplement 1. Statistical analyses of oogenesis onset in different**
850 **groups of animals on OP50 versus CS180.** GFP (+) and GFP (-) are animals that
851 expressed or did not express the oogenesis markers, *lin-41::GFP* or *oma-1::GFP*,
852 respectively. The **Figure 5** panels associated with the data are indicated. Significant p
853 values are shown in red and italicized. * denotes p values between OP50-fed worms
854 versus CS180-fed worms. # denotes experiments in which animals that carry the
855 *daf-2(e1368)* or *daf-2(e1370)* mutation and the corresponding controls were grown at
856 20°C and transferred to 25°C at the early L3 stage. All other experiments involved animals
857 that were continuously grown at 25°C.

858

859 **Figure 6. *ins-6* acts from ASJ neurons to promote early oogenesis. (A)**
860 *ins-6p::mCherry* transcriptional reporter *drcSi68* expression in ASI (n = 29, OP50; n = 29,
861 CS180) and ASJ (n = 30, OP50; n = 30, CS180) neurons during mid-to-late L3. **(B)**
862 *lin-41::GFP* expression in *ins-6(tm2416)* deletion mutants that were either rescued with:
863 (i) the wild-type *ins-6* genomic locus in two independent lines, *jxEx27* and *jxEx28*; (ii) ASI
864 neuron-specific expression of *ins-6*; or (iii) ASJ neuron-specific expression of *ins-6* in two
865 independent lines, *jxEx58* and *jxEx59*. **(C)** *lin-41::GFP* expression in the (i) *loxP-flanked*
866 *ins-6(syb7547)* homozygotes, (ii) *ins-6(tm2416)* homozygotes that carry the CRE
867 recombinase transgene that is specifically expressed in ASJ (ASJp::*CRE*), (iii)
868 *ins-6(tm2416)* heterozygotes that carry the ASJp::*CRE* transgene, (iv)
869 *ins-6(tm2416)*/*ins-6(syb7547)* transheterozygotes, and (v) animals in which *ins-6* was
870 deleted specifically from ASJ but remains present in ASI. * indicates $p \leq 0.05$; **, $p \leq 0.01$;
871 ***, $p \leq 0.001$; and leth, lethargus.

872 **Figure 6—supplement 1. Statistical analyses of oogenesis onset in different**
873 **groups of animals on OP50 versus CS180.** GFP (+) and GFP (-) are animals that
874 expressed or did not express the oogenesis marker *lin-41::GFP*, respectively. The **Figure**
875 **6** panels associated with the data are indicated. Significant p values are shown in red and
876 italicized. * denotes p values between OP50-fed worms versus CS180-fed worms.

877 **Figure 7. AWA olfactory neurons modulate food type-dependent fertilization rates,**
878 **but not early oogenesis onset. (A-B)** Sensory mutations influenced the food-type effects
879 on fertilization rates. **(C-I)** Animals that lack the sensory neurons ADF **(C)**, ASH **(D)**, ASI
880 **(E)**, ASK **(F)**, ASJ **(G)**, AWB **(H)**, and AWC **(I)**. **(J)** Animals lacking the sensory neuron
881 AWA in *odr-7* mutants. **(K)** Animals that lack both AWA and ASJ. Controls for **G** and **K**
882 carried the *ofm-1p::gfp* marker in the wild-type background. All other controls **(A-F, H-J)**
883 were wild-type worms. **(L)** Food type-dependent expression of the oogenesis reporter
884 *lin-41::GFP* in controls or animals lacking AWA and/or ASJ. ** indicates $p \leq 0.01$; ***, $p \leq$
885 0.001; and leth, lethargus.

886 **Figure 7—supplement 1. Statistical analyses of fertilization rates and**
887 **oogenesis onset in different sensory-impaired animals on OP50 versus CS180.**
888 Sheet 1 shows the analyses for fertilization rates before normalization; sheet 2, for
889 normalized fertilization rates; and sheet 3, for oogenesis onset in animals lacking AWA
890 and/or ASJ. On sheet 1, N is the total number of animals that were assayed. Means are
891 from pooled data from multiple, independent trials. SD is the standard deviation. On sheet
892 3, GFP (+) and GFP (-) are animals that expressed or did not express the *lin-41::GFP*
893 oogenesis marker, respectively. On all sheets, the **Figure 7** panels associated with the
894 data are indicated. Significant p values are shown in red and italicized. On sheets 1 and/or
895 3, the following abbreviation and superscripted letters denote: WT, wild type; NA, not
896 applicable; *A*, p values between a given strain grown on OP50 versus CS180 at each time
897 point; *B*, p values between a given strain grown on OP50 versus wild type on OP50; and
898 *C*, p values between a given strain grown on CS180 versus wild type on CS180.

899 **Figure 8. Insulin receptor signaling alter global fertilization rates independent of**
900 **food type. (A)** The weak reduction-of-function *daf-2(e1368)* mutant. **(B)** The strong
901 reduction-of-function *daf-2(e1370)* mutant. **(C-F)** *daf-16* null mutants and the three ILP
902 mutants, *ins-6*, *daf-28* or *ins-1*. Controls and *daf-2* mutants in **(A-B)** were shifted from 20°C
903 to 25°C as early L4s, whereas all other animals were continuously grown at 25ºC on OP50
904 (black closed circles for wild type; black closed triangles for the indicated mutants) or
905 CS180 (grey open circles for wild type; blue open triangles for the indicated mutants).

906 **Figure 8—supplement 1. Statistical analyses of fertilization rates in insulin**
907 **signaling-impaired animals on OP50 versus CS180.** Sheet 1 shows the analyses for
908 fertilization rates before normalization; and sheet 2, for normalized fertilization rates. N is
909 the total number of animals that were assayed. Means are from pooled data from multiple,
910 independent trials. SD is the standard deviation. The **Figure 8** panels associated with the
911 data are indicated. Significant p values are shown in red and italicized. [#] denotes
912 experiments in which animals that carry the *daf-2(e1368)* or *daf-2(e1370)* mutation and
913 the corresponding controls were grown at 20°C and transferred to 25°C at the early L4
914 stage. The following abbreviation and superscripted letters denote: WT, wild type; NA, not
915 applicable; *A*, p values between a given strain on OP50 versus CS180 at each time point;
916 *B*, p values between a given strain grown on OP50 versus wild type on OP50; and *C*, p
917 values between a given strain grown on CS180 versus wild type on CS180; *D*, p values
918 between a given strain versus the indicated ILP double or triple mutant on OP50; and *E*,
919 p values between a given strain versus the indicated ILP double or triple mutant on CS180.

920 **Figure 9. A model for the sensory modulation of food type-dependent oogenesis**
921 **onset and fertilization.** ILP INS-6 acts from ASJ neurons to promote early onset of
922 oogenesis. Olfactory neuron AWA promotes oocyte fertilization through mechanism(s)
923 distinct from DAF-2 insulin receptor signaling, which in turn regulates fertilization
924 independent of food type through the activities of other insulin-like peptide(s).

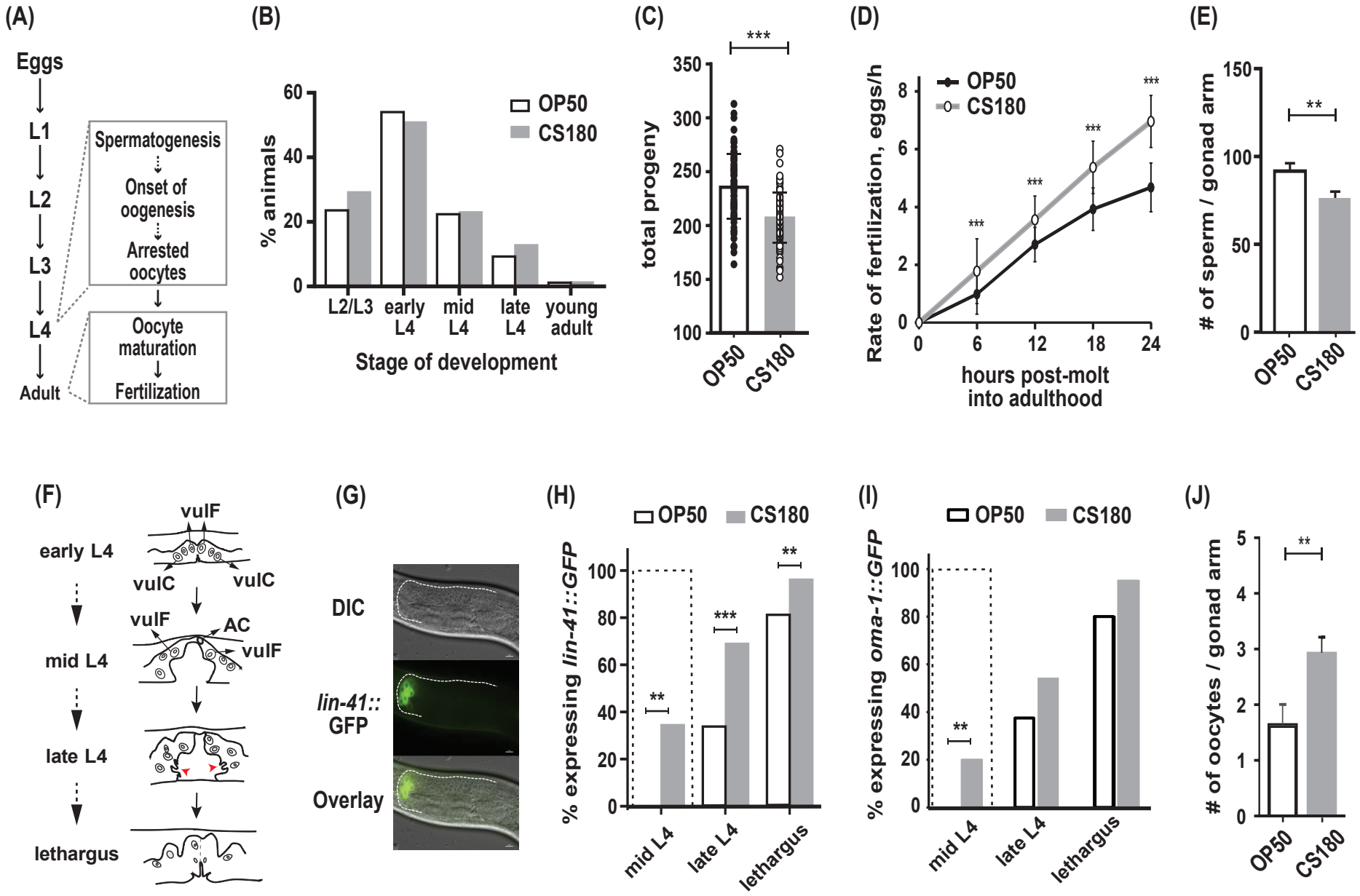
(A)
Eggs
L1
L2
L3
L4
Adult
Spermatogenesis
Onset of oogenesis
Arrested oocytes
Oocyte maturation
Fertilization
(B)
% animals
OP50
CS180
L2/L3
early L4
mid L4
late L4
young adult
Stage of development
(C)
total progeny
***
OP50
CS180
(D)
Rate of fertilization, eggs/h
OP50
CS180
hours post-molt into adulthood
(E)
# of sperm / gonad arm
**
OP50
CS180
(F)
early L4
mid L4
late L4
lethargus
vulF
vulC
AC
(G)
DIC
lin-41:: GFP
Overlay
(H)
OP50
CS180
% expressing lin-41::GFP
mid L4
late L4
lethargus
(I)
OP50
CS180
% expressing oma-1::GFP
mid L4
late L4
lethargus
(J)
# of oocytes / gonad arm
**
OP50
CS180

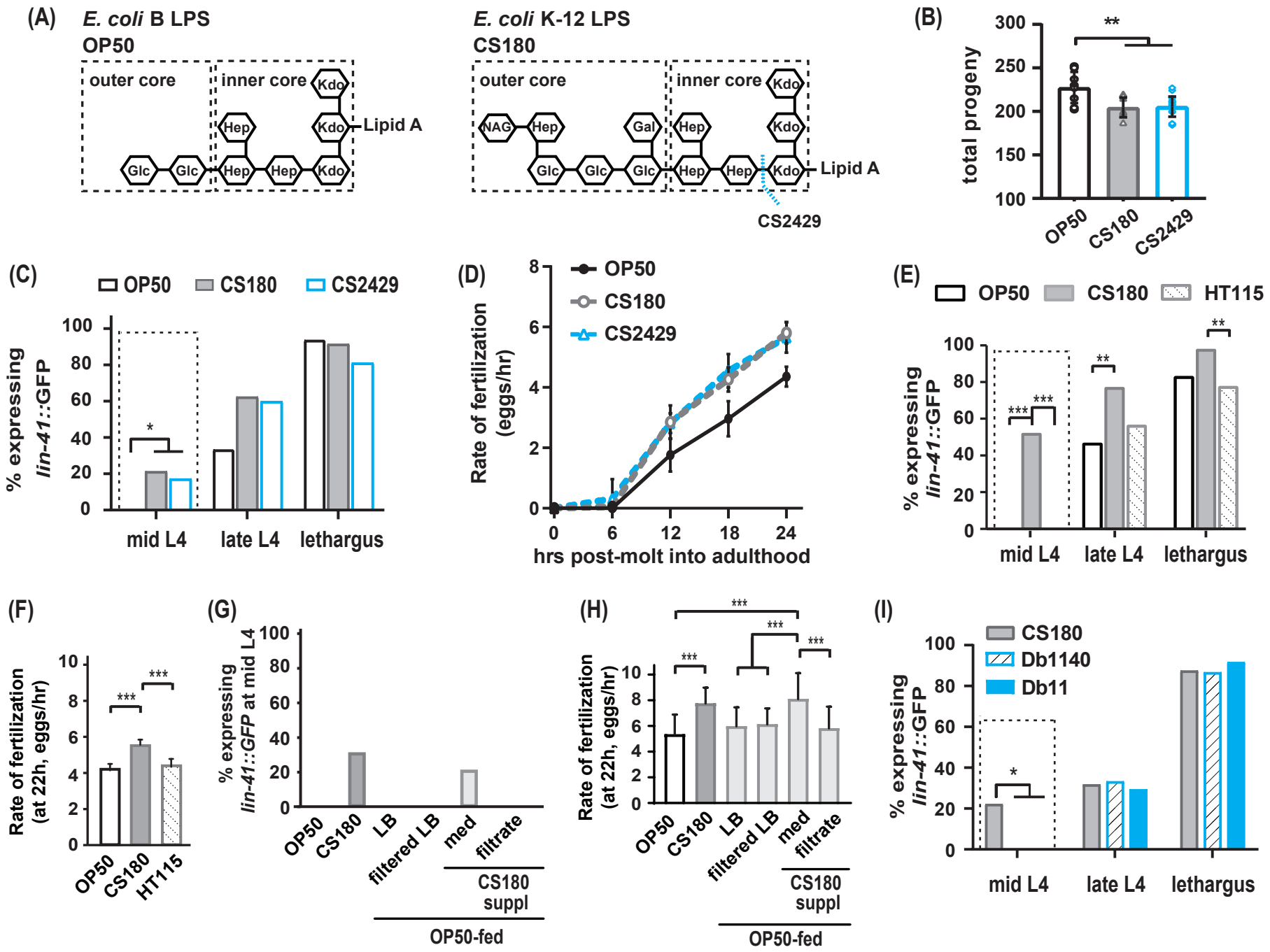
(A)
E. coli B LPS
OP50
outer core
inner core
Kdo
Hep
Kdo
Lipid A
Glc
Glc
Hep
Hep
Kdo
E. coli K-12 LPS
CS180
outer core
inner core
NAG
Hep
Gal
Hep
Kdo
Glc
Glc
Glc
Hep
Hep
Kdo
Lipid A
CS2429
(B)
total progeny
300
250
200
150
100
**
OP50
CS180
CS2429
(C)
OP50
CS180
CS2429
% expressing lin-41::GFP
100
80
60
40
20
0
*
mid L4
late L4
lethargus
(D)
OP50
CS180
CS2429
Rate of fertilization (eggs/hr)
8
6
4
2
0
0
6
12
18
24
hrs post-molt into adulthood
(E)
OP50
CS180
HT115
% expressing lin-41::GFP
100
80
60
40
20
0
***
***
**
**
mid L4
late L4
lethargus
(F)
Rate of fertilization (at 22h, eggs/hr)
10
8
6
4
2
0
***
***
OP50
CS180
HT115
(G)
% expressing lin-41::GFP at mid L4
100
80
60
40
20
0
OP50
CS180
LB
filtered LB
med
filtrate
CS180 suppl
OP50-fed
(H)
Rate of fertilization (at 22h, eggs/hr)
10
8
6
4
2
0
***
***
***
***
OP50
CS180
LB
filtered LB
med
filtrate
CS180 suppl
OP50-fed
(I)
CS180
Db1140
Db11
% expressing lin-41::GFP
100
80
60
40
20
0
*
mid L4
late L4
lethargus

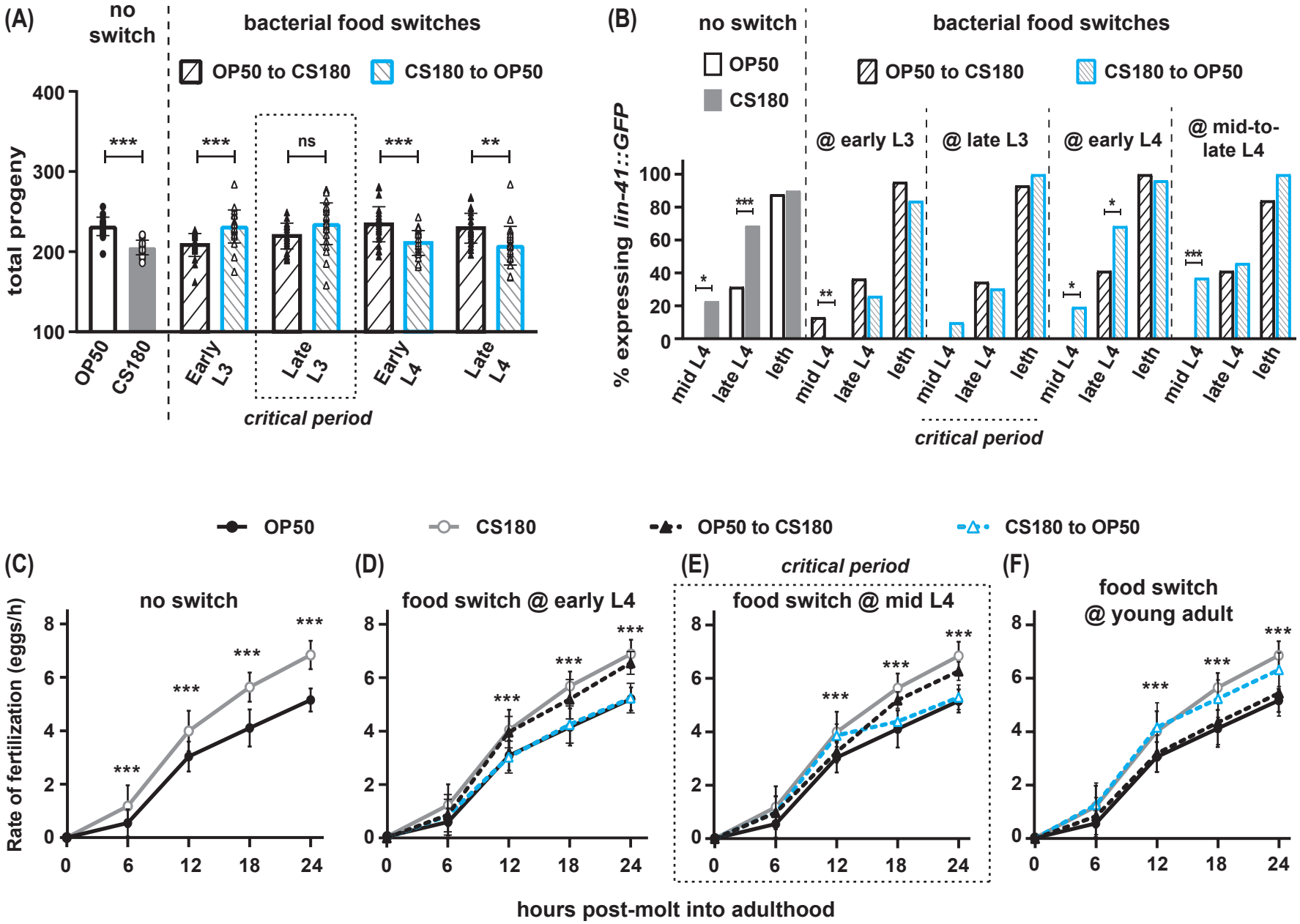
(A)
no switch
bacterial food switches
OP50 to CS180
CS180 to OP50
total progeny
400
300
200
100
***
***
ns
***
**
OP50
CS180
Early L3
Late L3
Early L4
Late L4
critical period
(B)
no switch
bacterial food switches
OP50
CS180
OP50 to CS180
CS180 to OP50
% expressing lin-41::GFP
@ early L3
@ late L3
@ early L4
@ mid-to-late L4
mid L4
late L4
leth
critical period
OP50
CS180
OP50 to CS180
CS180 to OP50
(C)
no switch
(D)
food switch @ early L4
(E)
critical period
food switch @ mid L4
(F)
food switch @ young adult
Rate of fertilization (eggs/h)
hours post-molt into adulthood

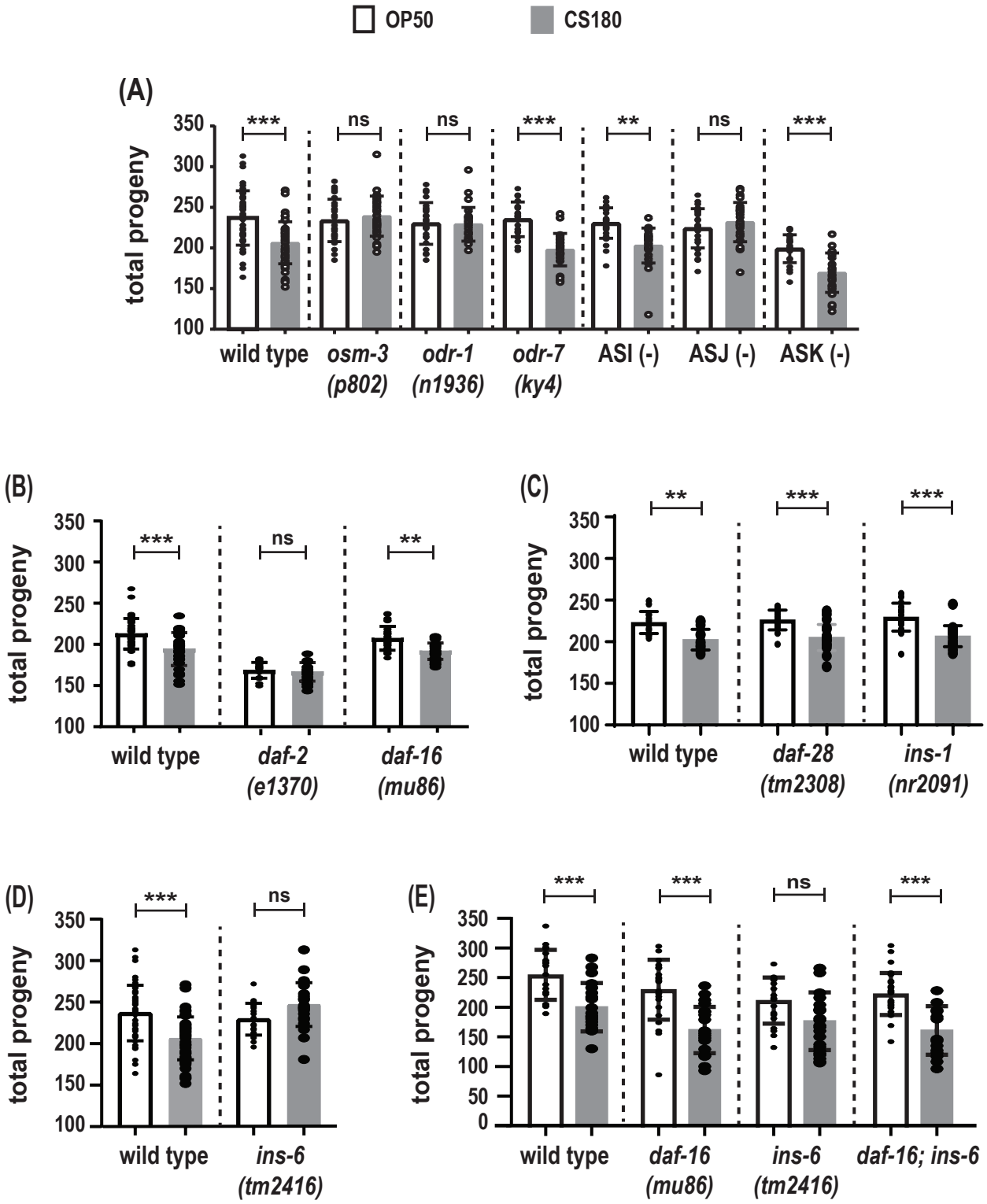
OP50
CS180
(A)
total progeny
350
300
250
200
150
100
***
ns
ns
***
**
ns
***
wild type
osm-3 (p802)
odr-1 (n1936)
odr-7 (ky4)
ASI (-)
ASJ (-)
ASK (-)
(B)
total progeny
***
ns
**
wild type
daf-2 (e1370)
daf-16 (mu86)
(C)
total progeny
**
***
***
wild type
daf-28 (tm2308)
ins-1 (nr2091)
(D)
total progeny
***
ns
wild type
ins-6 (tm2416)
(E)
total progeny
50
0
***
***
ns
***
wild type
daf-16 (mu86)
ins-6 (tm2416)
daf-16; ins-6

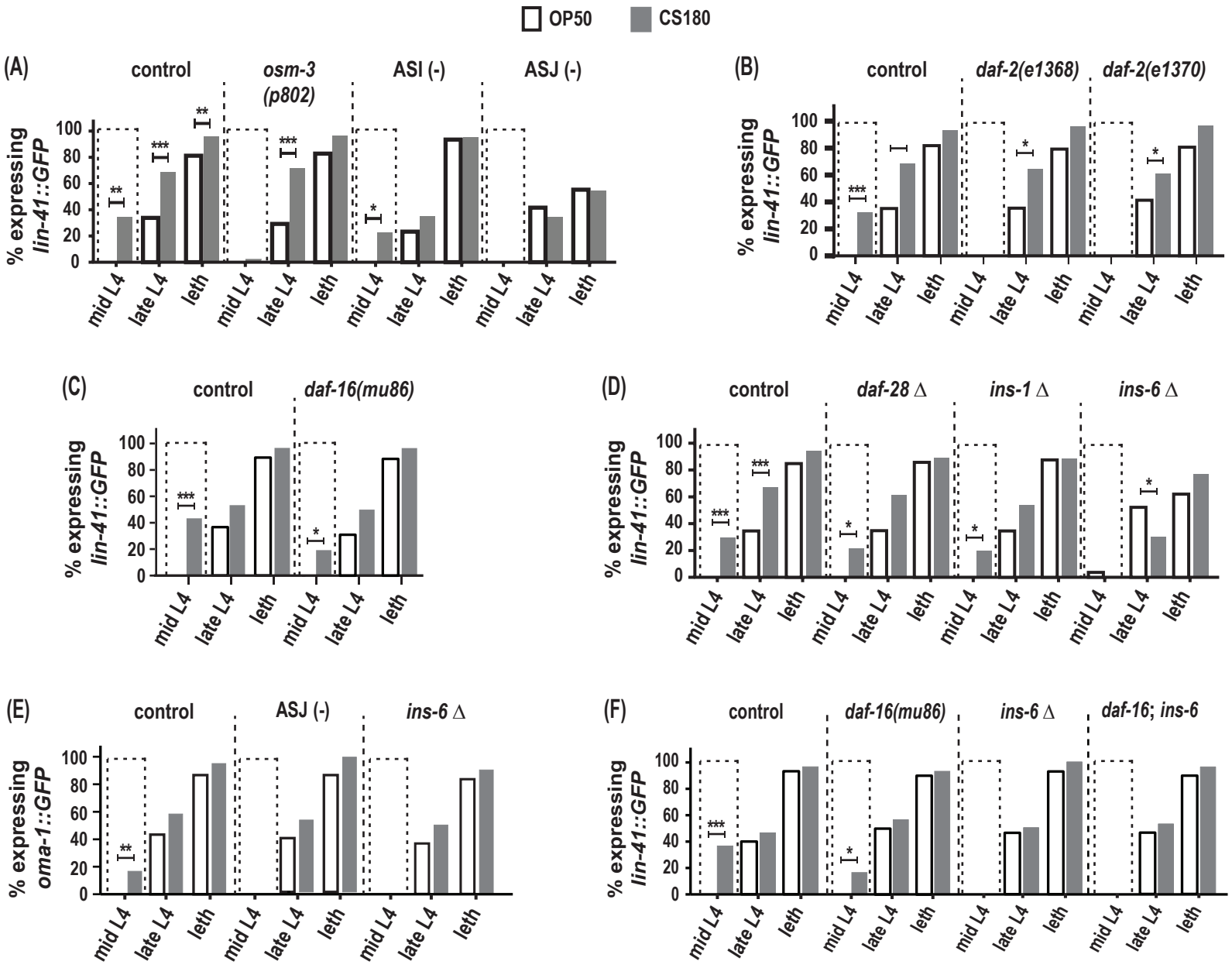
OP50
CS180
(A)
control
osm-3 (p802)
ASI (-)
ASJ (-)
% expressing lin-41::GFP
(B)
control
daf-2(e1368)
daf-2(e1370)
% expressing lin-41::GFP
(C)
control
daf-16(mu86)
% expressing lin-41::GFP
(D)
control
daf-28 Δ
ins-1 Δ
ins-6 Δ
% expressing lin-41::GFP
(E)
control
ASJ (-)
ins-6 Δ
% expressing oma-1::GFP
(F)
control
daf-16(mu86)
ins-6 Δ
daf-16; ins-6
% expressing lin-41::GFP
mid L4
late L4
leth

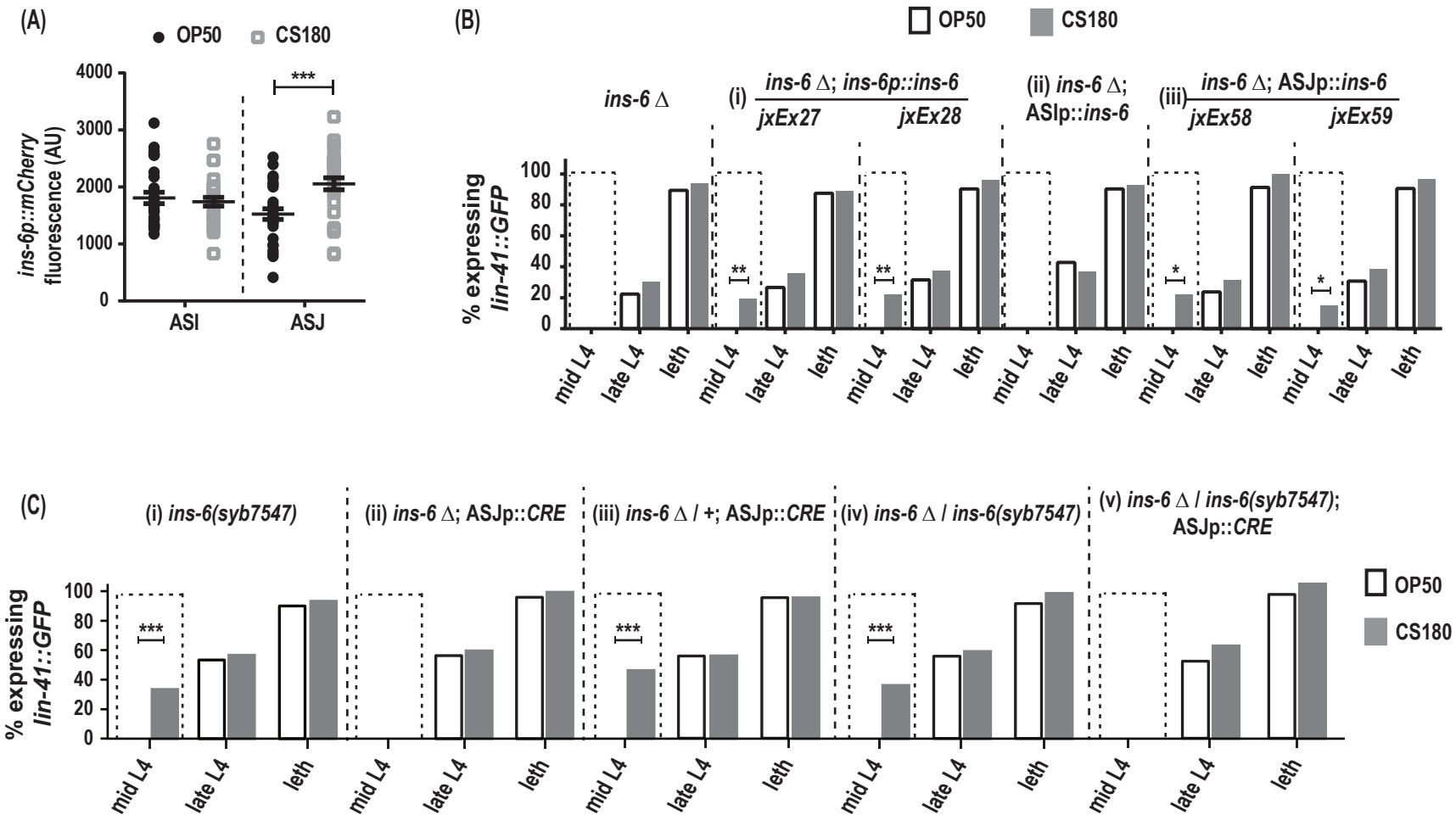
(A)
OP50
CS180
ins-6p::mCherry fluorescence (AU)
4000
3000
2000
1000
0
***
ASI
ASJ
(B)
OP50
CS180
ins-6 Δ
(i) ins-6 Δ; ins-6p::ins-6
jxEx27
jxEx28
(ii) ins-6 Δ; ASIp::ins-6
(iii) ins-6 Δ; ASJp::ins-6
jxEx58
jxEx59
% expressing lin-41::GFP
100
80
60
40
20
0
**
**
*
*
mid L4
late L4
leth
(C)
(i) ins-6(syb7547)
(ii) ins-6 Δ; ASJp::CRE
(iii) ins-6 Δ / +; ASJp::CRE
(iv) ins-6 Δ / ins-6(syb7547)
(v) ins-6 Δ / ins-6(syb7547); ASJp::CRE
% expressing lin-41::GFP
***
OP50
CS180

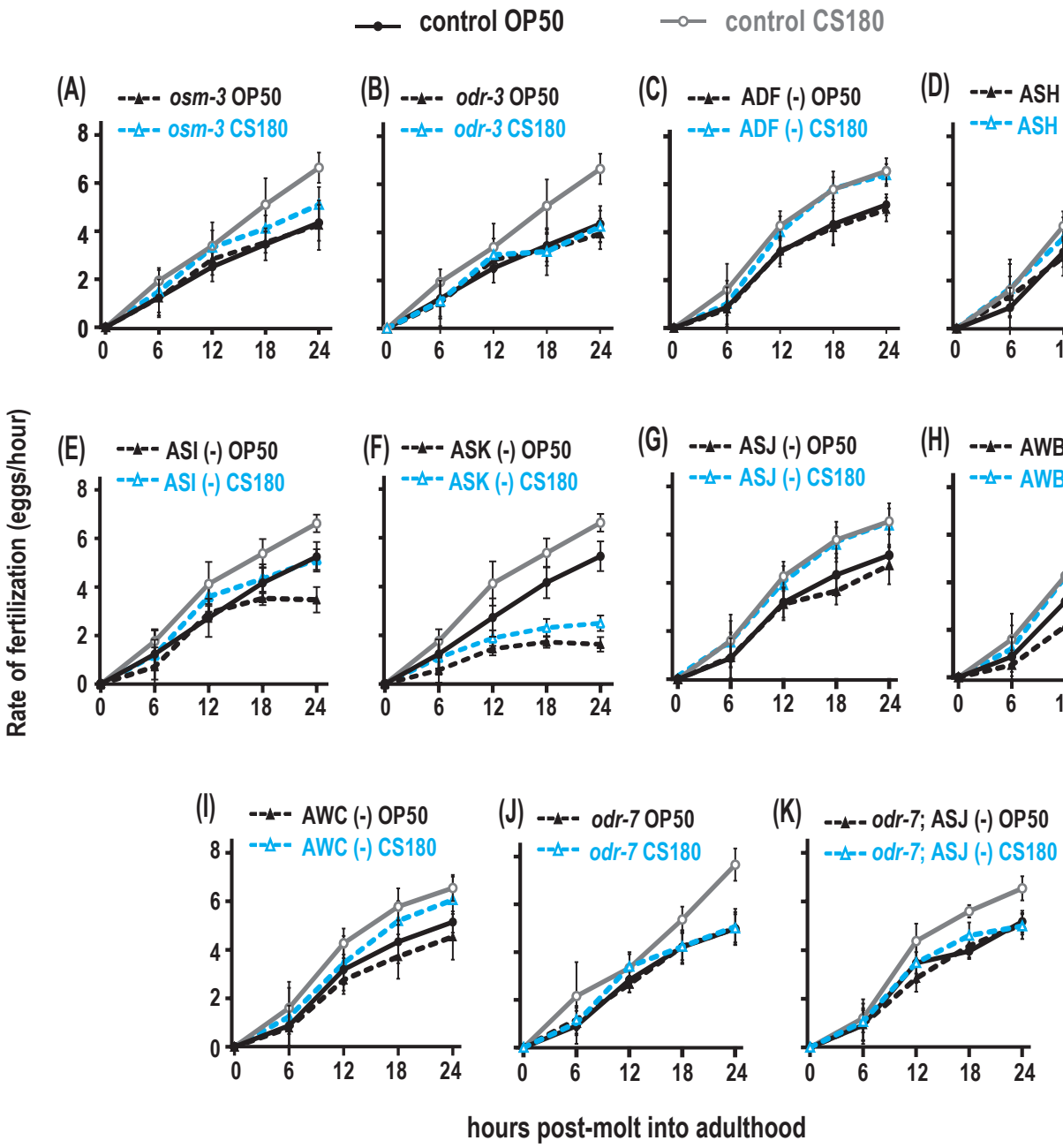
control OP50
control CS180
(A)
osm-3 OP50
osm-3 CS180
(B)
odr-3 OP50
odr-3 CS180
(C)
ADF (-) OP50
ADF (-) CS180
(D)
ASH (-) OP50
ASH (-) CS180
(E)
ASI (-) OP50
ASI (-) CS180
(F)
ASK (-) OP50
ASK (-) CS180
(G)
ASJ (-) OP50
ASJ (-) CS180
(H)
AWB (-) OP50
AWB (-) CS180
(I)
AWC (-) OP50
AWC (-) CS180
(J)
odr-7 OP50
odr-7 CS180
(K)
odr-7; ASJ (-) OP50
odr-7; ASJ (-) CS180
Rate of fertilization (eggs/hour)
hours post-molt into adulthood

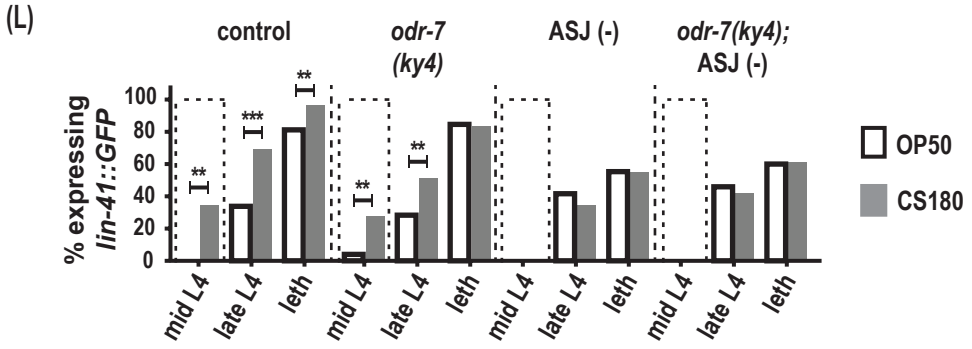
(L)
control
odr-7 (ky4)
ASJ (-)
odr-7(ky4); ASJ (-)
% expressing lin-41::GFP
mid L4
late L4
leth
OP50
CS180

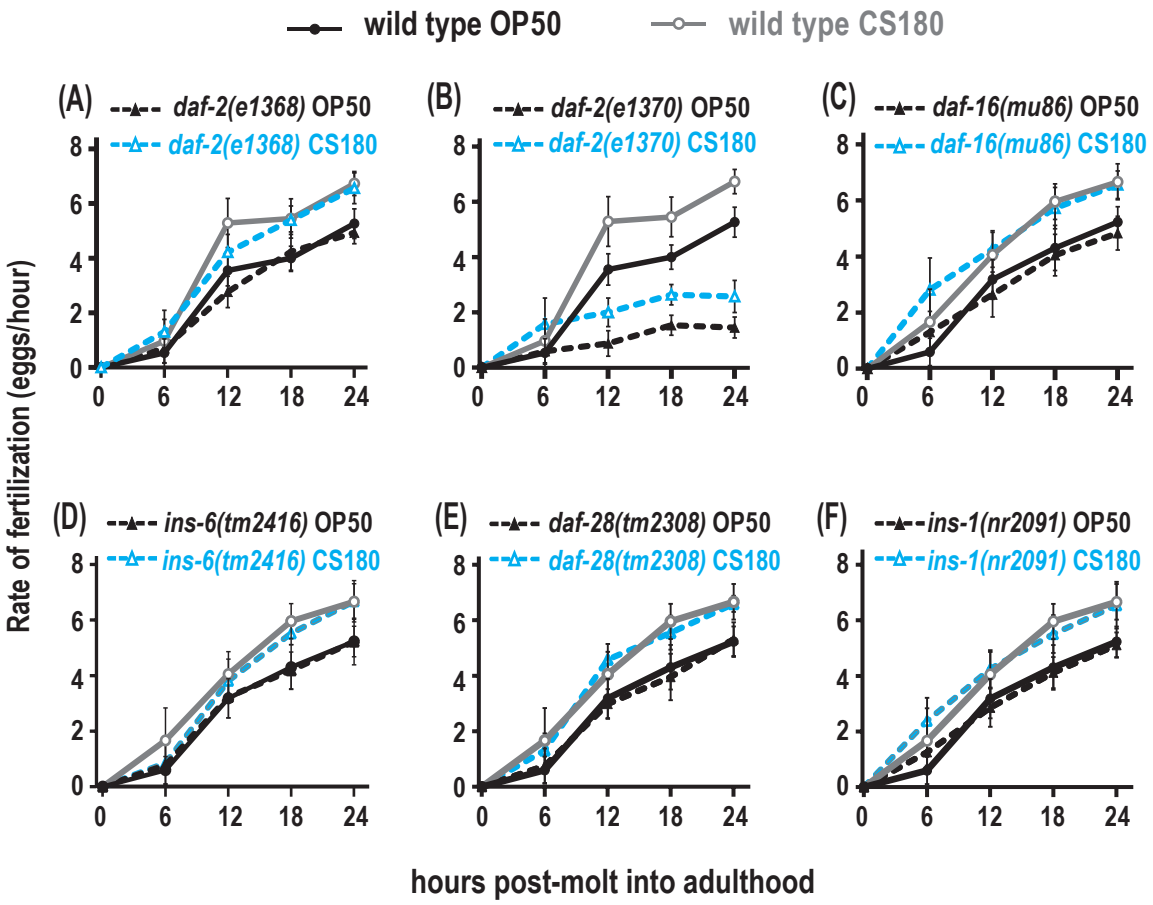
wild type OP50
wild type CS180
(A)
daf-2(e1368) OP50
daf-2(e1368) CS180
(B)
daf-2(e1370) OP50
daf-2(e1370) CS180
(C)
daf-16(mu86) OP50
daf-16(mu86) CS180
(D)
ins-6(tm2416) OP50
ins-6(tm2416) CS180
(E)
daf-28(tm2308) OP50
daf-28(tm2308) CS180
(F)
ins-1(nr2091) OP50
ins-1(nr2091) CS180
Rate of fertilization (eggs/hour)
hours post-molt into adulthood
0
2
4
6
8
0
6
12
18
24

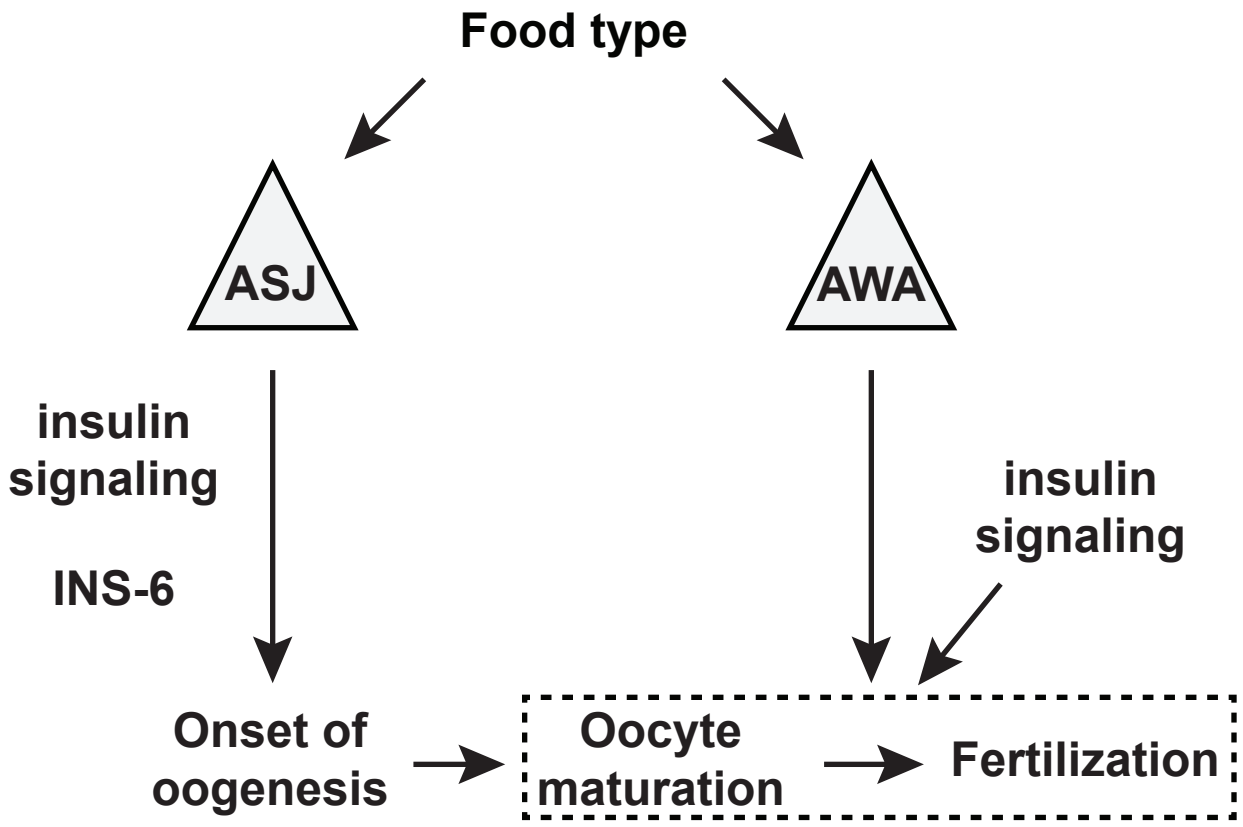
Food type
ASJ
AWA
insulin
signaling
INS-6
insulin
signaling
Onset of
oogenesis
Oocyte
maturation
Fertilization

Supplementary File 1. List of strains

Strain	Genotype	Reference(s)
Oogenesis marker, *lin-41::GFP*	*lin-41(tn1541[GFP::tev::s::lin-41])*	Spike et al., 2014
Oogenesis marker, *oma-1::GFP*	*unc-119(ed3); teIs1(oma-1::GFP + unc-119[+])*	Lin, 2003
Sensory mutants	*odr-1(n1936)*	L'Etoile and Bargmann, 2000
	odr-3(n1605)	Roayaie et al., 1998
	odr-10(ky225)	Sengupta et al., 1996
	osm-3(p802)	Tabish et al., 1995
	lin-41(tn1541); osm-3(p802)	This work
ADF (-)	*udEx211(srh-142::ced-3(p15); srh-142::ced-3(p17; srh-142::gfp; elt-2::gfp)*	Krzyzanowski et al., 2016
ASH (-)	*peIs1713(sra-6p::mCasp-1 + unc-122p::mCherry)*	Yoshida et al., 2012
ASI (-)	*oyIs84(gpa-4p::TU813 gcy-27p::TU814 gcy-27p::GFP coelp::dsRED)*	Beverly et al., 2011
	lin-41(tn1541); oyIs84	This work
ASJ (-)	*pgIs(trx-1p::ICE)*	Cornils et al., 2011; integrated by M. Goodman (gift)
	lin-41(tn1541); pgIs(trx-1p::ICE)	This work
	teIs1(oma-1::GFP + unc-119[+]); pgIs(trx-1p::ICE)	This work
ASK (-)	*qrIs2(sra-9::mCasp1)*	Srinivasan et al., 2012
AWA (-)	*odr-7(ky4)*	Sengupta et al., 1994
	lin-41(tn1541); odr-7(ky4)	This work
	Ex[odr-10::mCasp1 + myo-3::GFP]	Yoshida et al., 2012; Schiffer et al., 2020
AWB (-)	*peIs1715(str-1p::mCasp-1 + unc-122p::GFP)*	Yoshida et al., 2012
AWC (-)	*oyIs85(ceh-36p::TU#813 + ceh-36p::TU#814 + srtx-1p::GFP + unc-122p::DsRed)*	Beverly et al., 2011
ASJ (-); AWA(-)	*pgIs(trx-1p::ICE); odr-7(ky4)*	This work
	lin-41(tn1541); pgIs(trx-1p::ICE); odr-7(ky4)	This work
Insulin signaling mutants	*daf-2(e1368)*	Gems et al., 1998
	lin-41(tn1541); daf-2(e1368)	This work
	daf-2(e1370)	Gems et al., 1998
	lin-41(tn1541); daf-2(e1370)	This work
	daf-16(mu86)	Lin et al., 1997
	lin-41(tn1541) daf-16(mu86)	This work
	ins-1(nr2091)	Pierce et al., 2001
	lin-41(tn1541); ins-1(nr2091)	This work
	ins-6(tm2416)	Cornils et al., 2011
	lin-41(tn1541); ins-6(tm2416)	This work
	lin-41(tn1541) daf-16(mu86); ins-6(tm2416)	This work
	ins-6(tm2416); teIs1(oma-1::GFP + unc-119[+])	This work
	daf-28(tm2308)	Cornils et al., 2011
	lin-41(tn1541); daf-28(tm2308)	This work
	ins-6(tm2416); daf-28(tm2308)	Cornils et al., 2011
	ins-6(tm2416); ins-1(nr2091)	Cornils et al., 2011
	ins-1(nr2091); daf-28(tm2308)	Cornils et al., 2011
	ins-6(tm2416); ins-1(nr2091); daf-28(tm2308)	Cornils et al., 2011
***ins-6* full genomic rescue**	*lin-41(tn1541); ins-6(tm2416); jxEx27(ins-6p::ins-6 [2 ng/ul]; ofm-1::GFP [25 ng/ul])*	Cornils et al., 2011; this work
	lin-41(tn1541); ins-6(tm2416); jxEx28(ins-6p::ins-6 [2 ng/ul]; ofm-1::GFP [25 ng/ul])	Cornils et al., 2011; this work

Supplementary File 1. List of strains (continued)

Strain	Genotype	Reference(s)
***ins-6* ASI-specific rescue**	*lin-41(tn1541); ins-6(tm2416); jxEx51(str-3p::ins-6 [25 ng/ul]; ofm-1::GFP [25 ng/ul])*	Cornils et al., 2011; this work
***ins-6* ASJ-specific rescue**	*lin-41(tn1541); ins-6(tm2416); jxEx58(trx-1p::ins-6 [25 ng/ul]; ofm-1::GFP [25 ng/ul])*	Cornils et al., 2011; this work
	lin-41(tn1541); ins-6(tm2416); jxEx59(trx-1p::ins-6 [25 ng/ul]; ofm-1::GFP [25 ng/ul])	Cornils et al., 2011; this work
ins-6p::mCherry drcSi68	*ttTi5605 drcSi68(ins-6p::mCherry; Cb-unc-119[+])II*	This work
floxed *ins-6* locus	*lin-41(tn1541); ins-6(syb7547)*	This work
ASJ-specific *CRE*	*lin-41(tn1541); ins-6(tm2416); jxEx225(trx-1p::nCRE::unc-54 3'UTR [50 ng/ul] + unc-122p::GFP [25 ng/ul])*	This work

Supplementary references

Beverly, M., Anbil, S., and Sengupta, P. 2011. Degeneracy and neuromodulation among thermosensory neurons contribute to robust thermosensory behaviors in *Caenorhabditis elegans*. *J Neurosci* **31**: 11718-11727.

Cornils, A., Gloeck, M., Chen, Z., Zhang, Y., and Alcedo, J. 2011. Specific insulin-like peptides encode sensory information to regulate distinct developmental processes. *Development* **138:** 1183-1193.

Gems, D., Sutton, A.J., Sundermeyer, M.L., Albert, P.S., King, K.V., Edgley, M.L., Larsen, P.L., and Riddle, D.L. 1998. Two pleiotropic classes of *daf-2* mutation affect larval arrest, adult behavior, reproduction and longevity in *Caenorhabditis elegans*. *Genetics* **150:** 129-155.

Krzyzanowski, M.C., Woldemariam, S., Wood, J.F., Chaubey, A.H., Brueggemann, C., Bowitch, A., Bethke, M., L'Etoile, N.D., and Ferkey, D.M. 2016. Aversive behavior in the nematode *C. elegans* is modulated by cGMP and a neuronal gap junction network. *PLoS Genet* **12:** e1006153.

L'Etoile, N.D., and Bargmann, C.I. 2000. Olfaction and odor discrimination are mediated by the *C. elegans* guanylyl cyclase ODR-1. *Neuron* **25:** 575-586.

Lin, K., Dorman, J.B., Rodan, A., and Kenyon, C. 1997. *daf-16*: An HNF-3/forkhead family member that can function to double the life-span of *Caenorhabditis elegans*. *Science* **278:** 1319–1322.

Lin R. 2003. A gain-of-function mutation in *oma-1*, a *C. elegans* gene required for oocyte maturation, results in delayed degradation of maternal proteins and embryonic lethality, *Dev Biol* **258**: 226-239.

Pierce, S.B., Costa, M., Wisotzkey, R., Devadhar, S., Homburger, S.A., Buchman, A.R., Ferguson, K.C., Heller, J., Platt, D.M., Pasquinelli, A.A*., et al.* 2001. Regulation of DAF-2 receptor signaling by human insulin and *ins-1*, a member of the unusually large and diverse *C. elegans* insulin gene family. *Genes Dev* **15:** 672-686.

Roayaie, K., Crump, J.G., Sagasti, A., and Bargmann, C.I. 1998. The G alpha protein ODR-3 mediates olfactory and nociceptive function and controls cilium morphogenesis in *C. elegans* olfactory neurons. *Neuron* **20:** 55-67.

Schiffer, J.A*.,* Servello, F.A., Heath, W.R., Amrit, F.R.G., Stumbur, S.V., Eder, M., Martin, O.M.F., Johnsen, S.B., Stanley, J.A., Tam, H*., et al.* 2020. *Caenorhabditis elegans* processes sensory information to choose between freeloading and self-defense strategies. *eLife* **9:** e56186.

Sengupta, P., Chou, J.H., and Bargmann, C.I. 1996. *odr-10* encodes a seven transmembrane domain olfactory receptor required for responses to the odorant diacetyl. *Cell* **84:** 899-909.

Sengupta, P., Colbert, H.A., and Bargmann, C.I. 1994. The *C. elegans* gene *odr-7* encodes an olfactory-specific member of the nuclear receptor superfamily. *Cell* **79:** 971-980.

Spike, C.A., Coetzee, D., Eichten, C., Wang, X., Hansen, D., and Greenstein, D. 2014. The TRIM-NHL protein LIN-41 and the OMA RNA-binding proteins antagonistically control the prophase-to-metaphase transition and growth of *Caenorhabditis elegans* oocytes. *Genetics* **198:** 1535-1558.

Srinivasan, J., von Reuss, S.H., Bose, N., Zaslaver, A., Mahanti, P., Ho, M.C., O'Doherty, O.G., Edison, A.S., Sternberg, P.W., and Schroeder, F.C. 2012. A modular library of small molecule signals regulates social behaviors in *Caenorhabditis elegans*. *PLoS Biol* **10:** e1001237.

Tabish, M., Siddiqui, Z.K., Nishikawa, K., and Siddiqui, S.S. 1995. Exclusive expression of *C. elegans osm-3* kinesin gene in chemosensory neurons open to the external environment. *J Mol Biol* **247:** 377-389.

Yoshida, K., Hirotsu, T., Tagawa, T., Oda, S., Wakabayashi, T., Iino, Y., and Ishihara, T. 2012. Odour concentration-dependent olfactory preference change in *C. elegans*. *Nat commun* **3:** 739.